

Quantum-enhanced measurements exploiting spatial-resolving-detectors



EUROPEAN
METROLOGY
NETWORKS

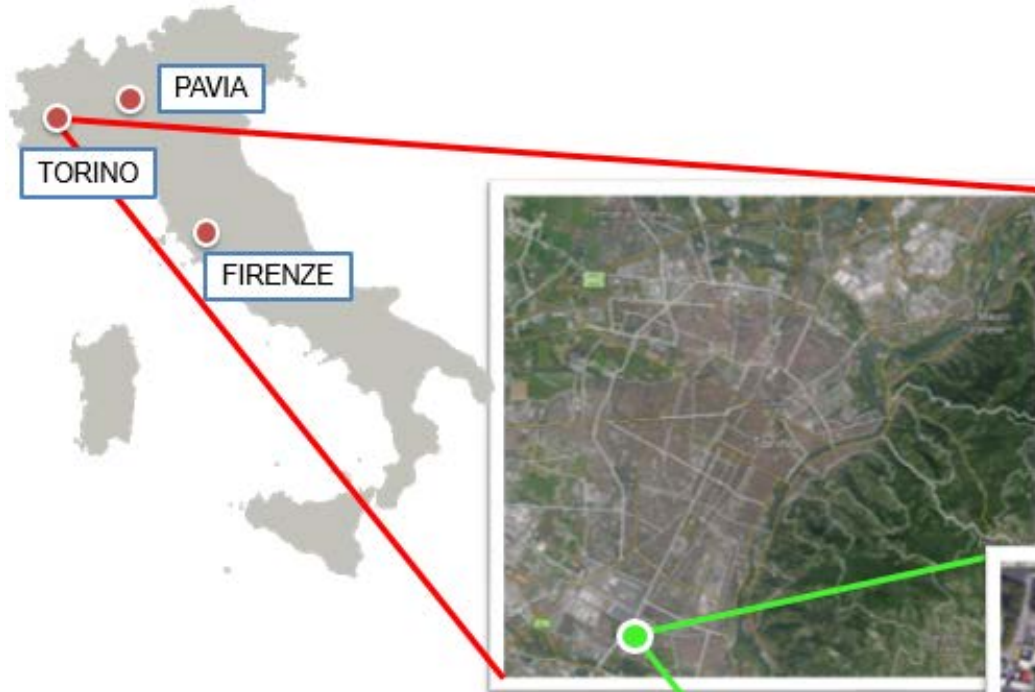


QUANTUM
TECHNOLOGIES



Ivo Pietro DEGIOVANNI
INRIM & EMN-Q Chair & INFN

INRIM IN A NUTSHELL



Three Scientific Divisions:

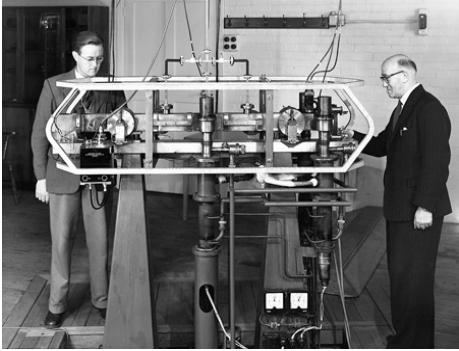
- Quantum Metrology and Nanotechnology
- Applied Metrology and Engineering
- Advanced Materials and Life Science

INRIM - the Italian National Metrological Institute

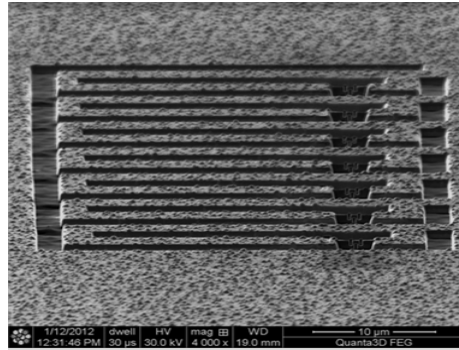
- More than 200 employees, 30 M€ annual account
- 4th NMI in Europe (account/employers)
- Strong relationship Academia and Industry
- Calibration Service
- Located in Turin, Pavia, and Florence



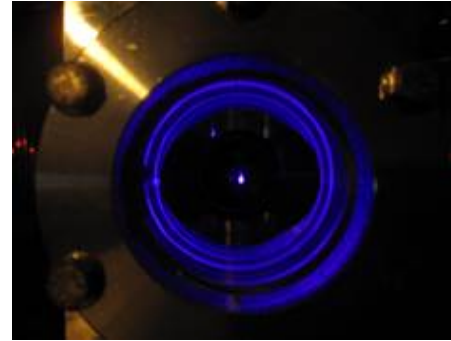
Quantum Metrology: shortest hystory



1967:
Time is the first SI unit
quantum-based

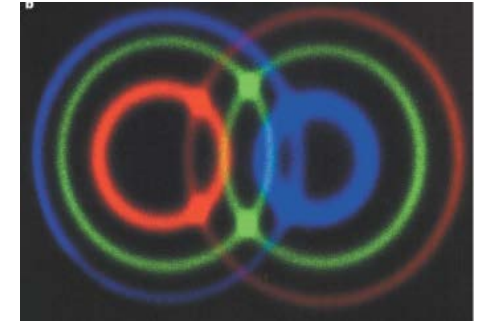


1975-1990:
Electrical units go
quantum: Josephson
effect, Hall effect, single-
electron tunnelling



1990-2020:
Laser cooling and
quantum optics: game
changers for the
measurements accuracy.

Nanostructured
materials open new
opportunities

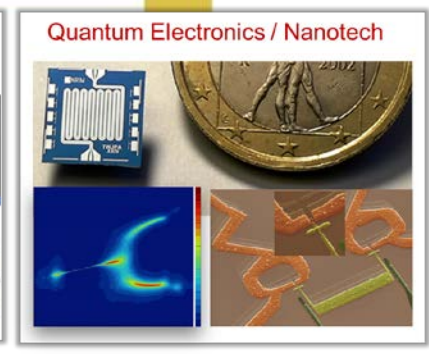
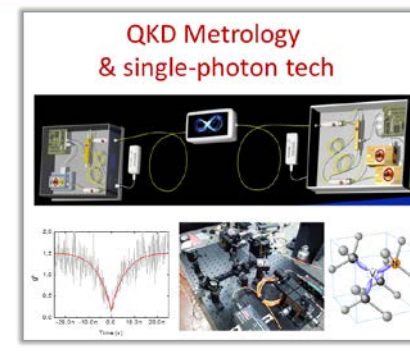
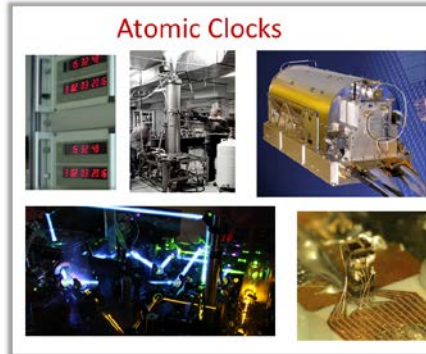


Today:
Nanophotonics,
Entanglement,
Atoms-on-a-chip
Metamaterials and
nanostructures are the
game changers in
metrology and sensing

INRIM IN A NUTSHELL

Quantum Metrology and Nanotechnology Division

Physics Chemistry and Nanotechnology
Quantum Electronics
Quantum Optics & Photometry
Time and Frequency



ITALIAN QUANTUM BACKBONE – 1850 Km

QKD IN-FIELD: first implementations

1. Test in field Turin-Santhù Inter-MAN (100 km, -30 dB)
 ✓ *Already done*
2. MAN Florence (17 km, -10 dB)
 Ongoing - Collaboration CNR (see Zavatta's talk)
3. MAN in Turin Area *in progress*
4. Interoperation Space-Ground in Matera *in progress* (collaboration with ASI)
5. Submarine environment: Malta-Sicily
 Done, follow up

- Quantum Technologies**
 - Radioastronomy
 - Ultracold atoms Physics
 - Space - Galileo
 - Finance
- 7 Research Institutes Involved:
 - CNR - National Research Council
 - ASI - Italian Space Agency
 - INAF - Italian Astrophysics Institute
- 4 Industrial Users:
 - Thales Alenia Space-Italy
 - Telespazio, Consortium Top-IX
 - Leonardo Valley

A complete platform for QKD
Components
Methods
Metrology and Standardisation
In-field Test
Implementation
Security of QKD

Metrology for QKD and QT

- Develop suitable metrics for
 - single photon sources
 - photon counting detectors
- Develop methods and measurement facilities for characterising non-classical properties of light:
 - antibunching
 - indistinguishability
 - entanglement
 - quantumness

Characterisation of optical components in QKD system

- Single-Photon sources
- Single Photon detectors
- Quantum hacking countermeasures, Q-encoders and Q-RNG

EuroQCI: European Quantum Communication Infrastructure Initiative

OQTAVO study for EuroQCI

A consortium of European digital players design the future EU quantum internet

The European Commission has selected a consortium of companies and research institutes to study the design of the European quantum communication network, EuroQCI (European Quantum Communication Infrastructure). It will enable ultra-secure communication between critical infrastructures and institutions across the European Union.

INRIM: representatives at the Expert Committee

Standardisation of QKD



EURAMET EMN for Quantum Technologies: EMN-Q



**EUROPEAN
METROLOGY
NETWORKS**

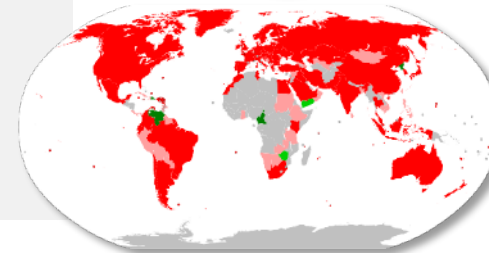


**QUANTUM
TECHNOLOGIES**

International Metrology and EURAMET

National Metrology Institutes (NMIs)

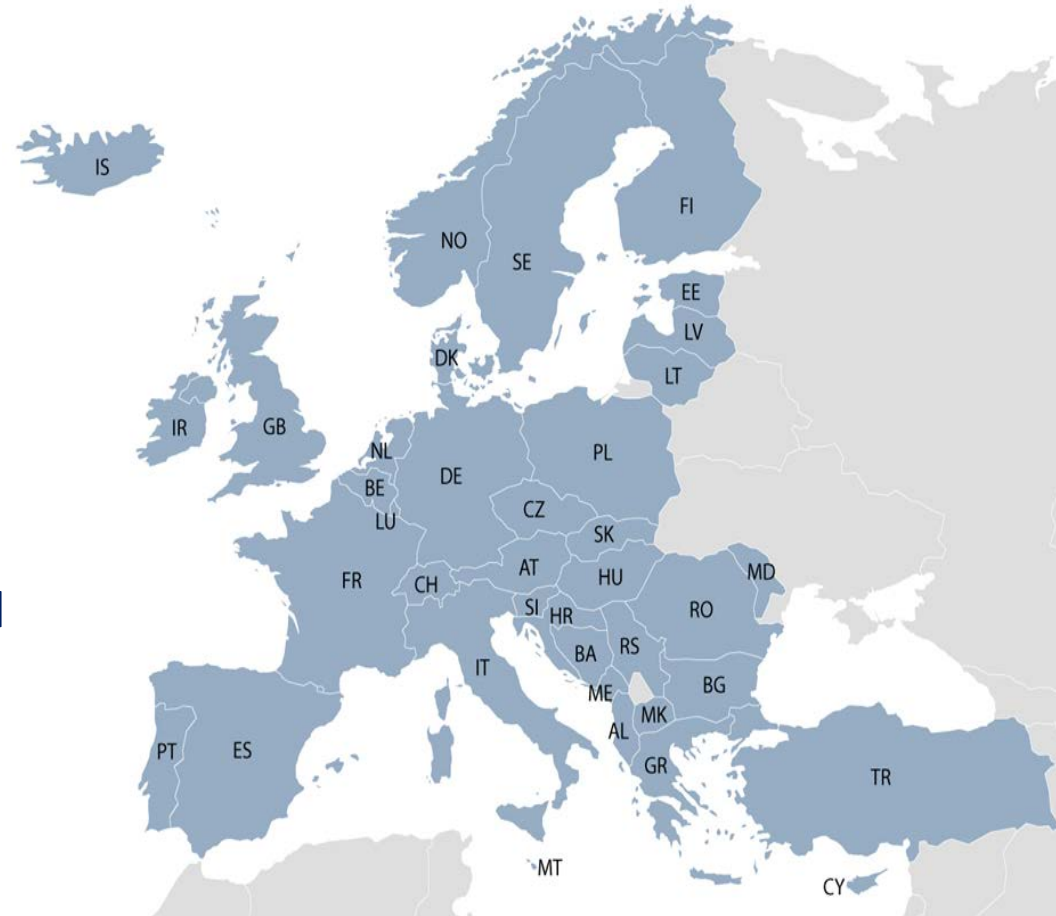
- ... develop and maintain metrology infrastructure **worldwide** in response to the needs from science, industry and society. Their core mission includes
 - cutting-edge measurement research, and
 - sustainable capabilities for measurement, calibration, testing and conformity assessment.
- ... harmonise and quality-assure their capabilities under the **Metre Convention:**
International treaty, established in 1875 to ensure measurement conformity between countries (initially 17, now more than 60).



International Metrology and EURAMET

EURAMET, the Regional Metrology Organisation (RMO) of Europe

- **38 National Metrology Institutes (Members)**
- **77 Designated Institutes (Associates)**
- **16 international Liaison Organisations** (e.g. IAEA, BIPM, WMO, EA, Eurachem, Eurolab)
- Providing stakeholders with **world-leading measurement solutions and standards**
- Securing **world-wide trust and acceptance** of measurements, for all aspects of business and society
- Implementing **Metrology Research Programmes**



EMN for Quantum Technologies: EMN-Q

EMN-Q Strategic Agenda (22 Oct. 2020)

Rationale

- **To align with industrial requirements, those of the EC Quantum Technologies Flagship, national and inter-governmental quantum technology (QT) programmes, and of any relevant stakeholders;**
- **to contribute to QT developments** through NMI's and DI's research and innovation activities;
- **to give input into the **standardisation & certification** of QT;**
- **to promote of the benefits of metrology to the stakeholders.**

Vision

EMN-Q aims at being the recognised European unique reference point representing European metrology for Quantum Technologies.

Today, EMN-Q has **18 EURAMET Members and Partners** from 15 countries.

Outline

Quantum Optics with Spatial Resolving Detector @ INRIM

- ... with CCD
- ... with Single-photon confocal microscope
- ... with SPAD arrays

Quantum Optics Group @INRIM

Since 1998 ...

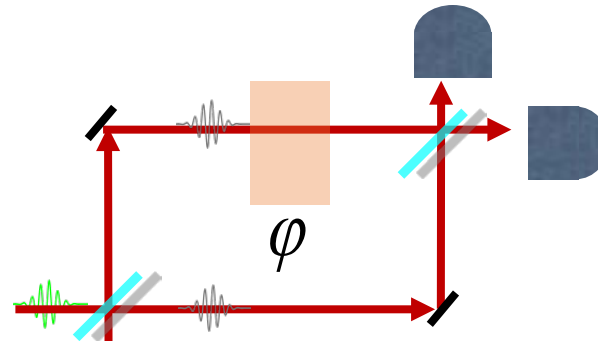


<https://quantum-optics.inrim.it/home-page>

Quantum Enhanced Measurement

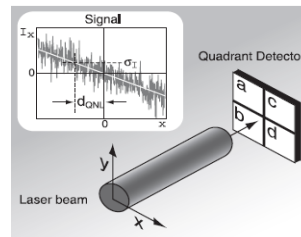
The Shot-Noise Limit

- phase
- Interferometry
- GW detectors



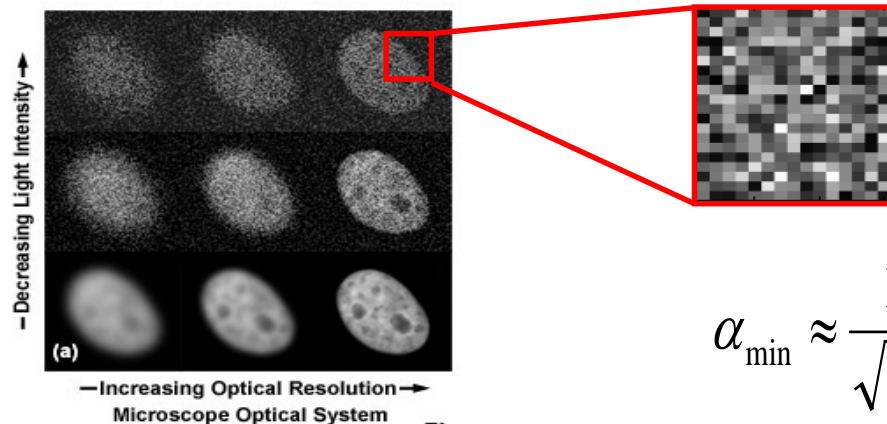
$$\Delta\varphi_{\min} \approx \frac{1}{\sqrt{N}}$$

- Displacement:
- lithography
- beams, particles tracking



$$X_R \approx \lambda \frac{f}{D} \quad \Delta x_{\min} \approx \frac{X_R}{\sqrt{N}}$$

- Absorption/reflection:
- Imaging
- microscopy
- Target recognition



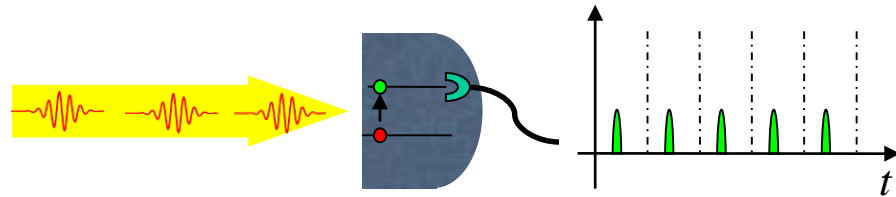
$$\alpha_{\min} \approx \frac{1}{\sqrt{N}}$$

Quantum Enhanced Measurement

However quantum mechanics predicts existence of quantum states of light which allow to beat the shot-noise limit

Fock state $|N\rangle$

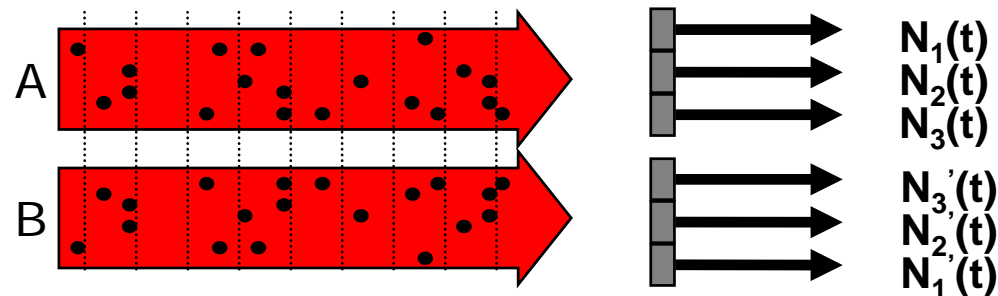
Single photon source : $|1\rangle$



$$\Delta N \approx 0 !!!$$

non-classical correlation and entanglement :

Twin beam:
$$|\Psi_{AB}^{(TWB)}\rangle = \prod_{\mathbf{k}} \left[\sum_n C_{\mathbf{k}}(n) |n_{\mathbf{k}}\rangle_A |n_{-\mathbf{k}}\rangle_B \right]$$



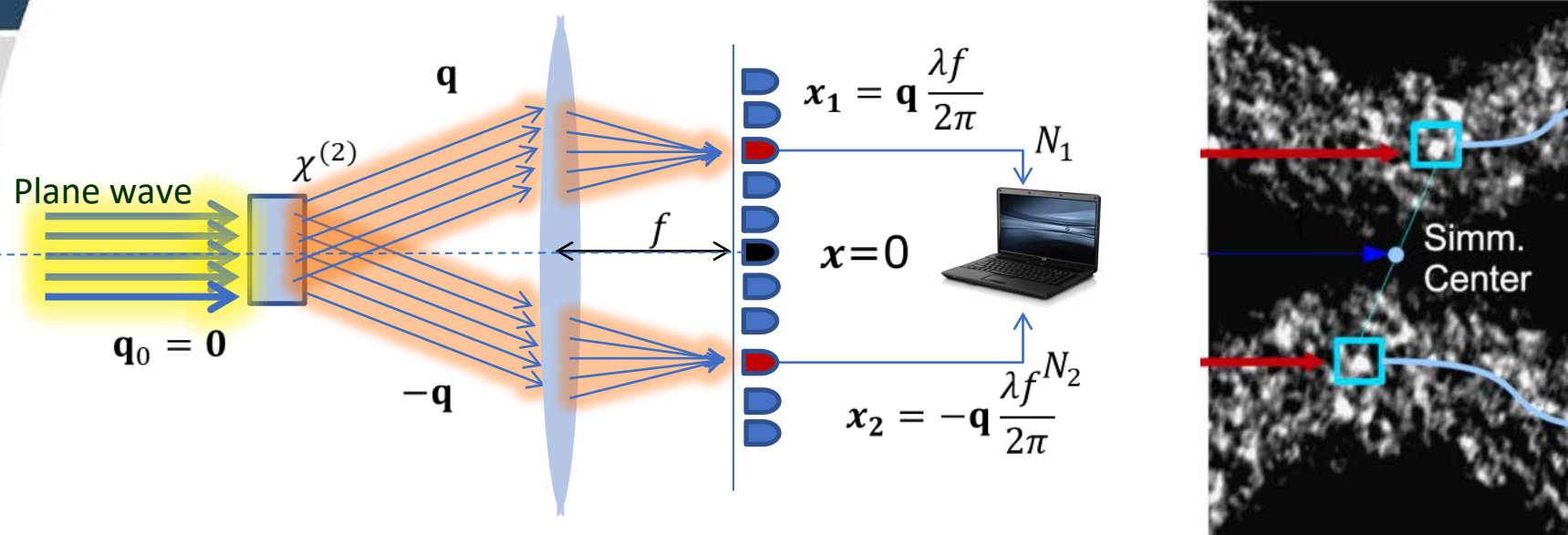
$$\sigma = \frac{\text{Var}(N_i - N'_i)}{\langle N_i + N'_i \rangle} < 1$$



QUANTUM

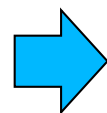


Quantum Enhanced Measurement



- Parametric Down Conversion: spontaneous decay of a pump photon in a photon pair (energy and momentum conservation).
- Transverse momentum conservation $\mathbf{q}_0 = \mathbf{q}_1 + \mathbf{q}_2$ implies photon pairs propagate along correlated directions.
- In the Far Field plane waves are focused in points \rightarrow Two point-like detectors would detect perfect two-modes quantum correlation (both in low and high gain regime)

$$\sigma = \frac{\text{Var}(N_1 - N_2)}{\langle N_1 + N_2 \rangle} = 1 - \eta < 1$$

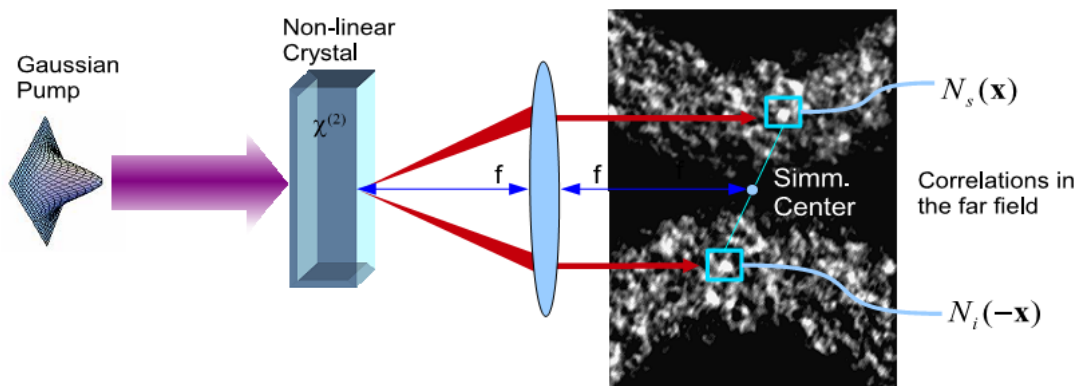


NON-CLASSICAL

CCD camera calibration

[Optics Expr. **18**, 20572 (2010); APL **105**, 10113 (2014); Opt. Lett. **41**, 1841 (2016)]

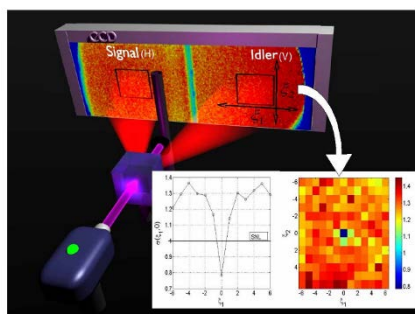
Bright Multimode Twin-Beams used to calibrate scientific CCD camera



$$|\psi(\mathbf{q})\rangle = \sum_n C_{\mathbf{q}}(n) |n\rangle_{i,\mathbf{q}} |n\rangle_{s,-\mathbf{q}}$$

$$\text{NRF: } \sigma \equiv \frac{\langle \delta^2 N_- \rangle}{\langle N_i + N_s \rangle}$$

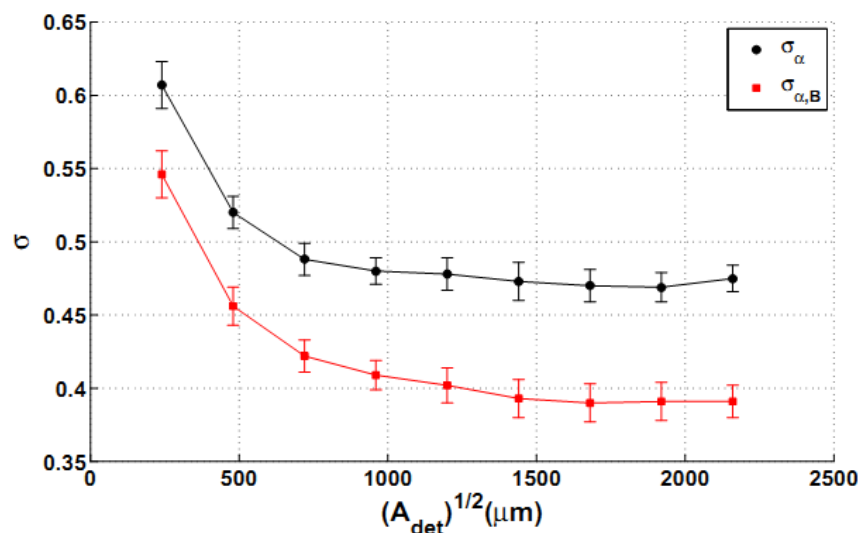
$$\langle \delta^2 N_- \rangle \equiv \langle \delta^2 N_s \rangle + \langle \delta^2 N_i \rangle - 2 \langle \delta N_i \delta \bar{N}_s \rangle$$



Corrected NRF

$$\sigma_{\alpha} \equiv \frac{\langle \delta^2 (N_s - \alpha N_i) \rangle}{2 \langle N_s \rangle} = \frac{1}{2} (1 + \alpha) - \eta_s$$

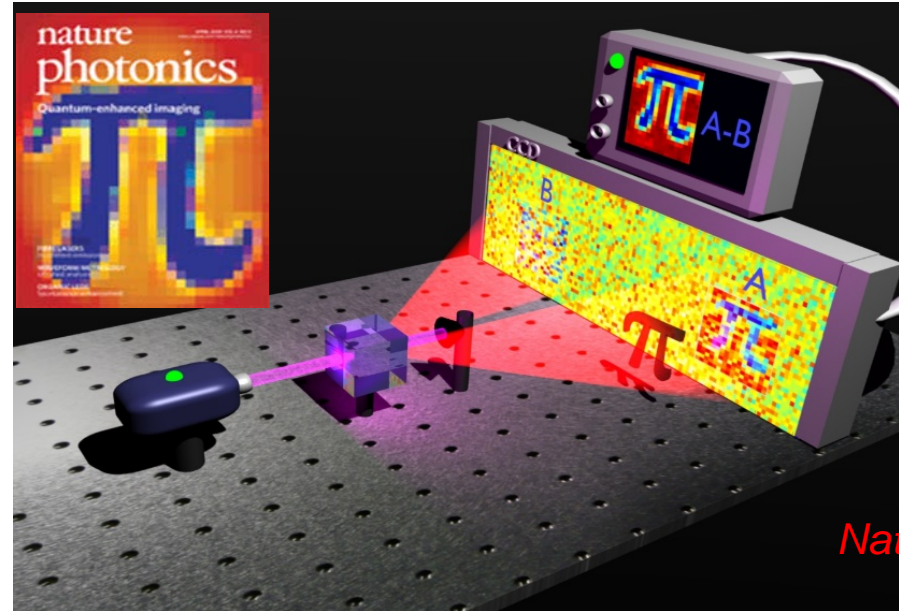
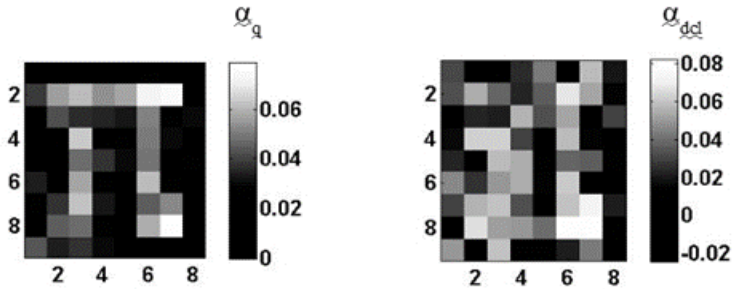
$$\alpha = \langle N_s \rangle / \langle N_i \rangle$$



Sub-Shot-Noise Imaging

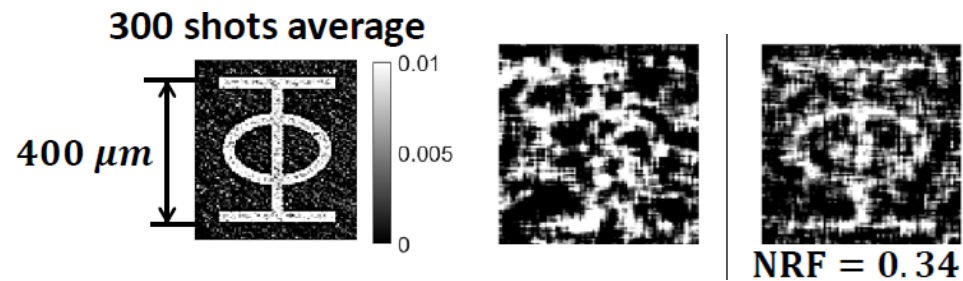
Sub-Shot Noise Imaging

Beating the shot-noise with quantum light



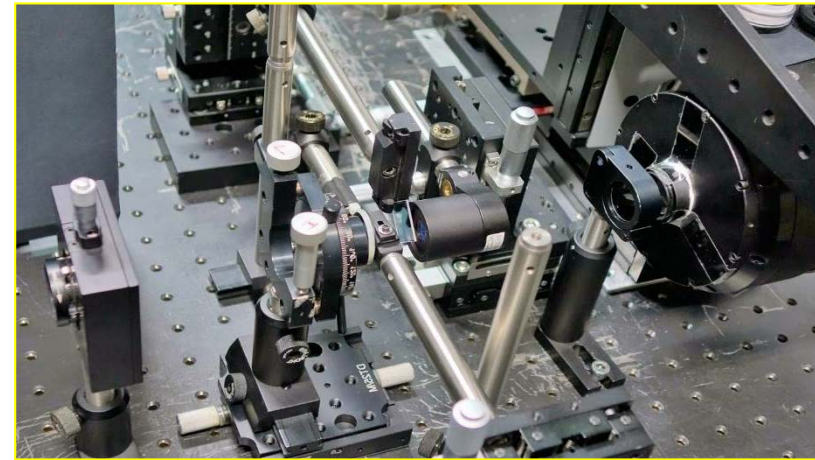
Nat. Photonics 4, 227 (2010)

Wide-Field Sub-Shot Noise Microscope



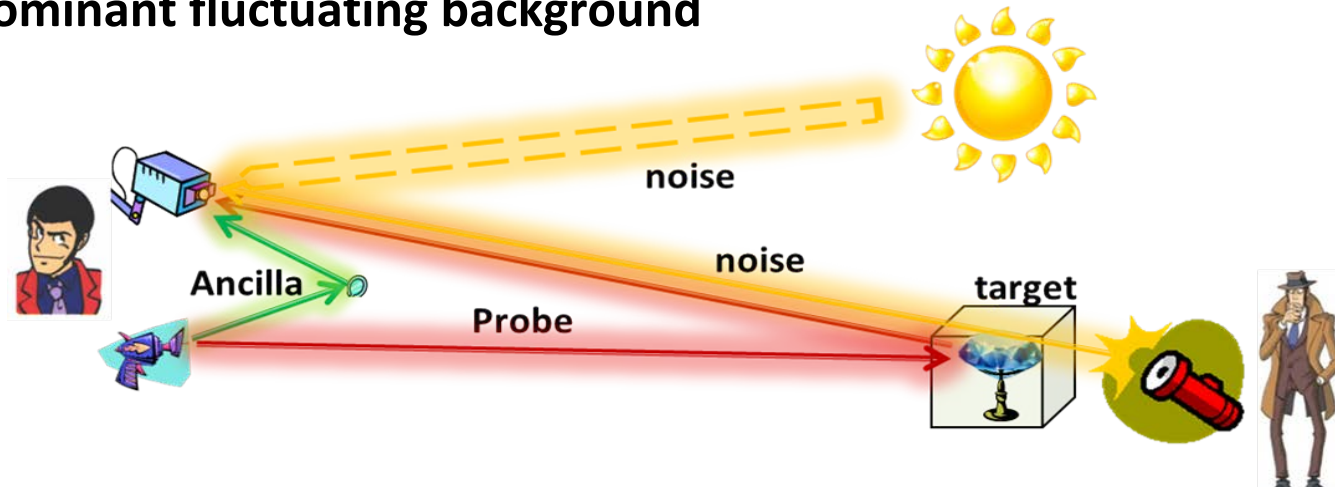
5 μm resolution

Light S&A 6, e17005 (2017)



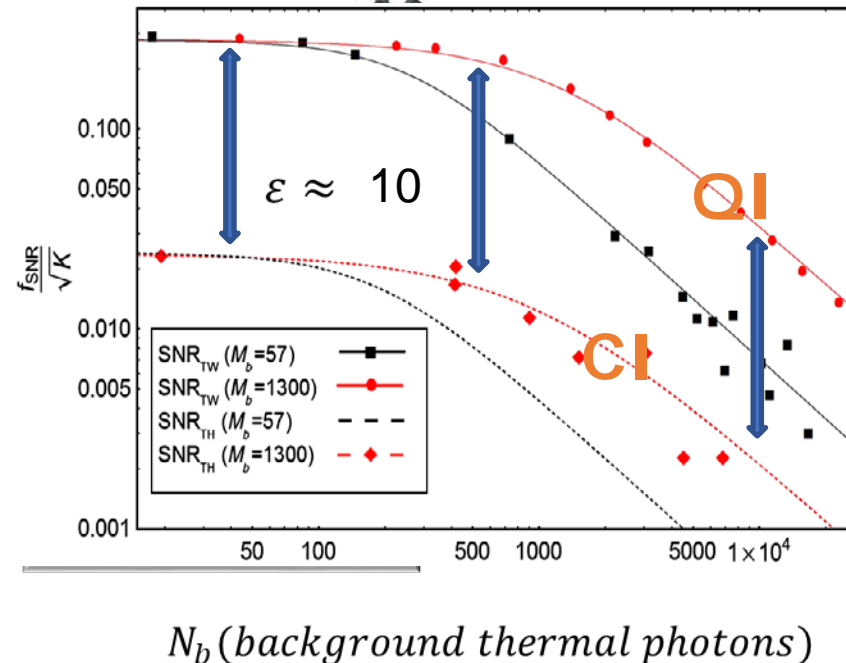
Quantum Illumination

Problem: detection of a partially reflecting target which is immersed in a dominant fluctuating background



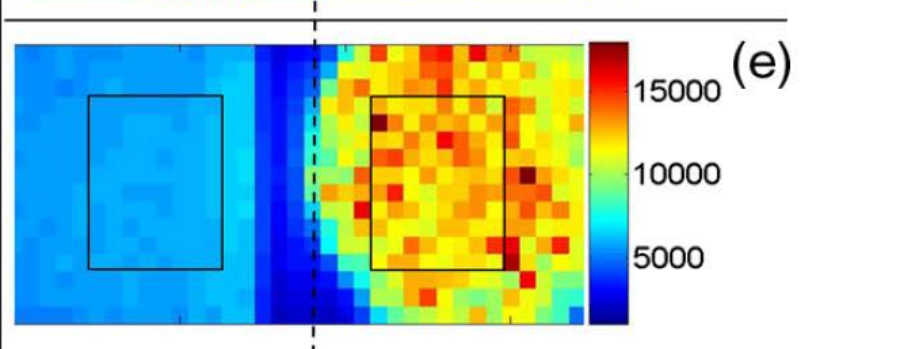
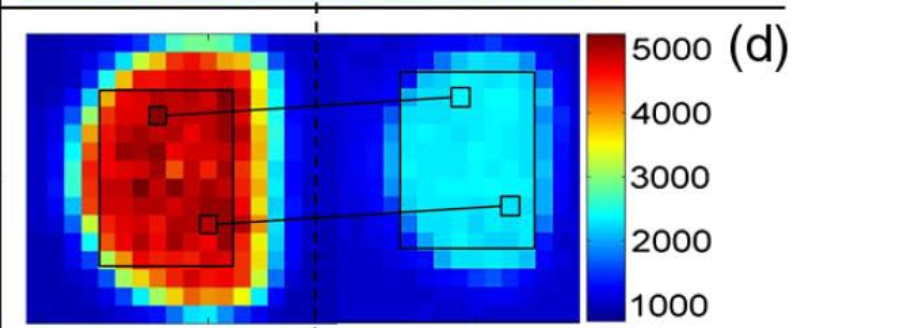
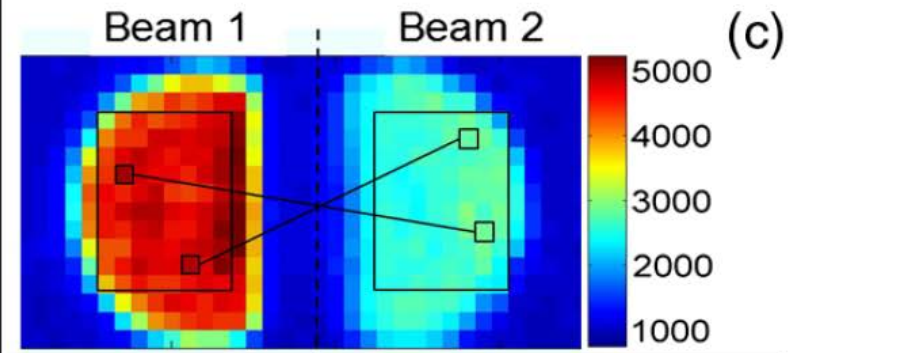
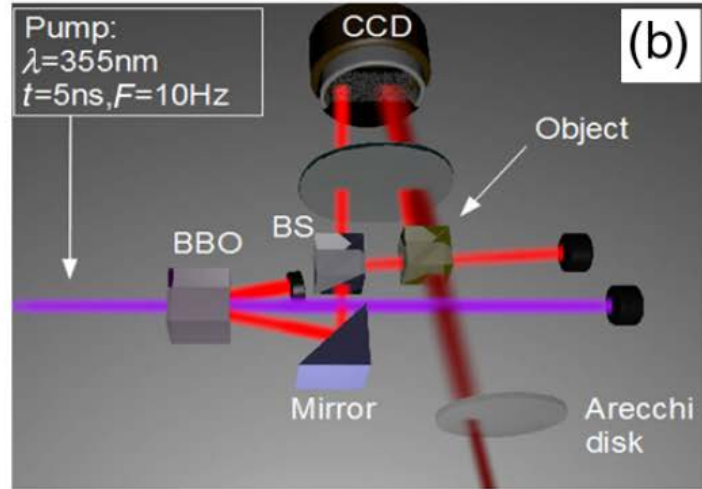
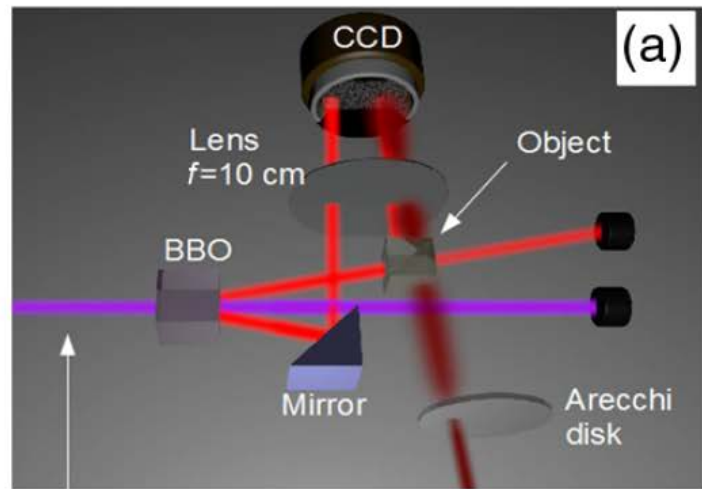
Quantum illumination takes advantage of an ancillary beam, quantum correlated /entangled with the probe, by a joint measurement of the two.

- ✓ **Large quantum enhancement!**
- ✓ **Independent of noise and losses!**
- ✓ **Non-classical signature does not survive the noise**

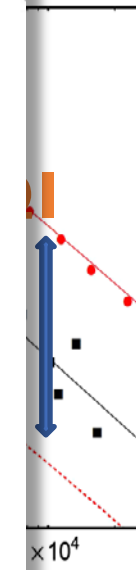


Quantum Illumination

Problem: detection of a partially reflecting target which is immersed in a dominant fluctuating background

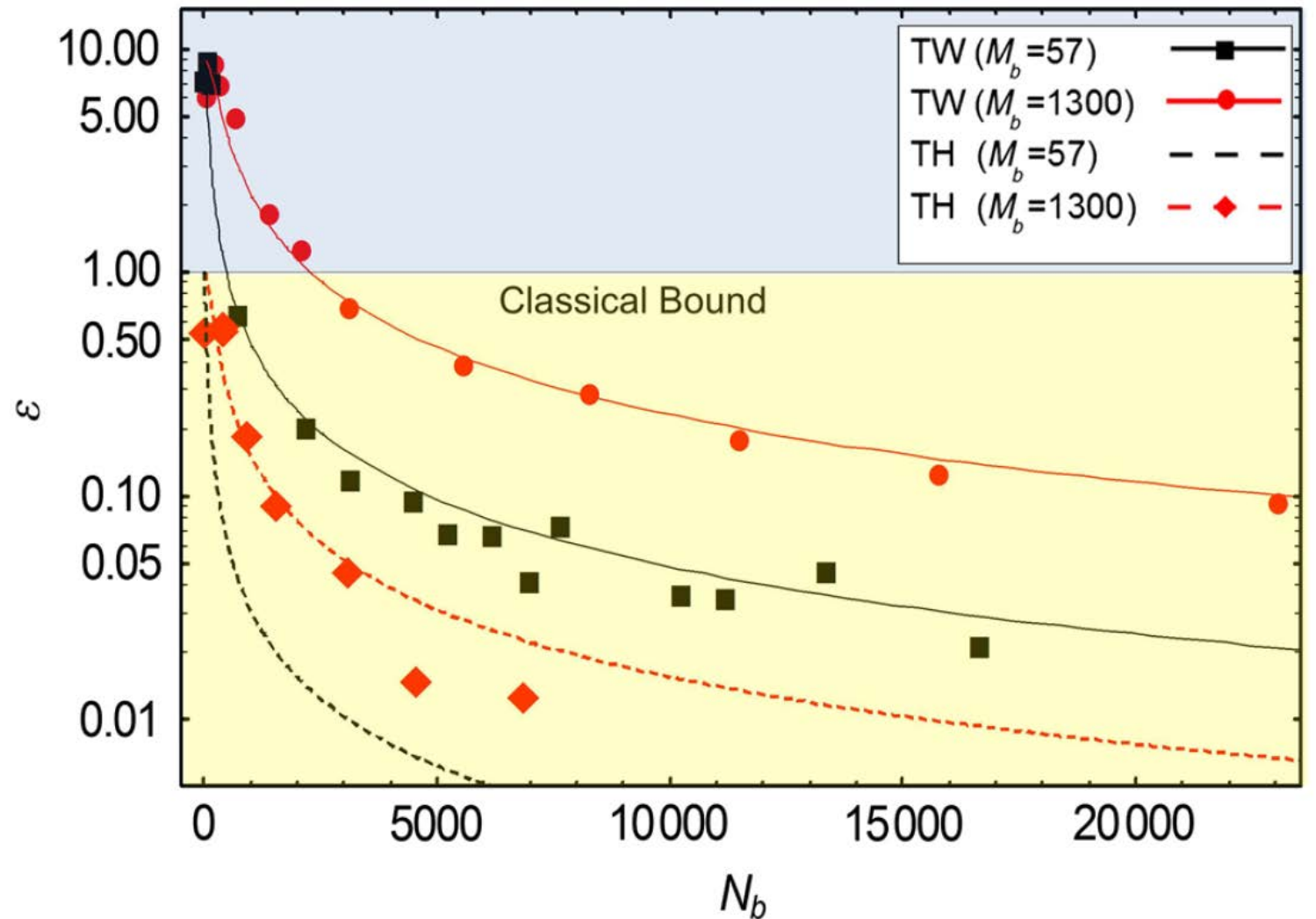
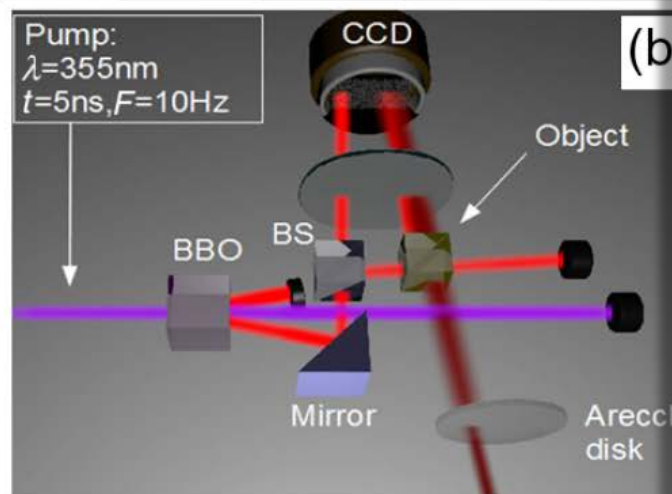
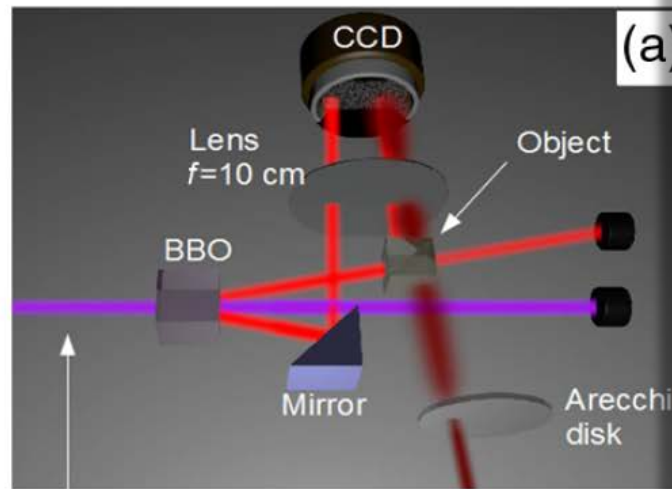


et al, PRL 110, 153603 (2013)



Quantum Illumination

Problem: detection of a partially reflecting target which is immersed in a dominant fluctuating background



Quantum Conformance Test (Reading)

Quantum Hypothesis Testing

Physical process \mathcal{P}_x producing a quantum object (the SUT \mathcal{E}_τ)

The process \mathcal{P}_x described by the ensemble $\{g_x(\tau), \mathcal{E}_\tau\}$

$g_x(\tau)$ probability distribution defines the SUT \mathcal{E}_τ

The **conformance test** consists in ruling whether an unknown process should be labeled

- “reference” process \mathcal{P}_0
- “defective” process \mathcal{P}_1

• **False negative** p_{10} : a SUT produced by a conform process ($x = 0$) is labeled as defective ($y = 1$):
An economic loss for a manufacturer when a conform process is considered defective. We will

• **False positive** p_{01} : a SUT produced by a defective process ($x = 1$) is labeled as conform ($y = 0$):
This outcome represents a risk since possibly unsafe products are released.

$$p_{err} = (p_{01} + p_{10})/2$$

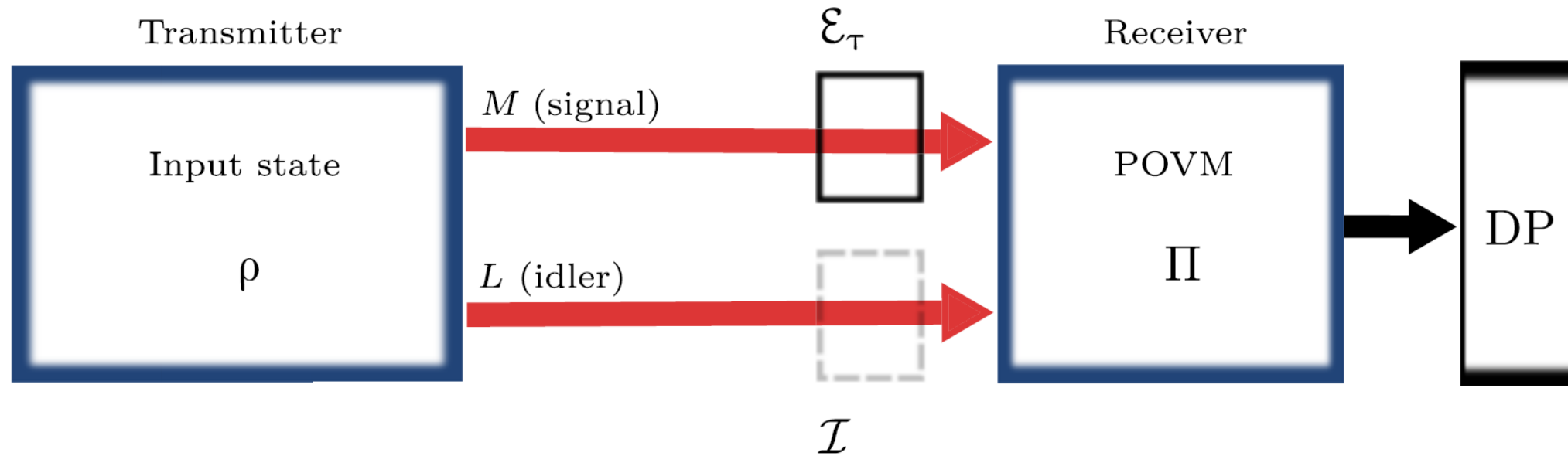
Ortolano et al., Sci. Adv.7, eabm3093 (2021)
Ortolano et al., Sci. Adv.7, eabc7796 (2021)



QUANTUM
TECHNOLOGIES



Quantum Conformance Test (Reading)



$$\rho_0 = \mathbb{E}_{\mathcal{P}_0}[(\mathcal{E}_\tau \otimes \mathcal{I})\rho] \rightarrow \text{reference process}$$

$$\rho_1 = \mathbb{E}_{\mathcal{P}_1}[(\mathcal{E}_\tau \otimes \mathcal{I})\rho] \rightarrow \text{defective process}$$

$D(\rho_0, \rho_1) = \|\rho_0 - \rho_1\|/2$ is the trace distance

$$p_{\text{err}} = \frac{1}{2}(1 - D(\rho_0, \rho_1))$$

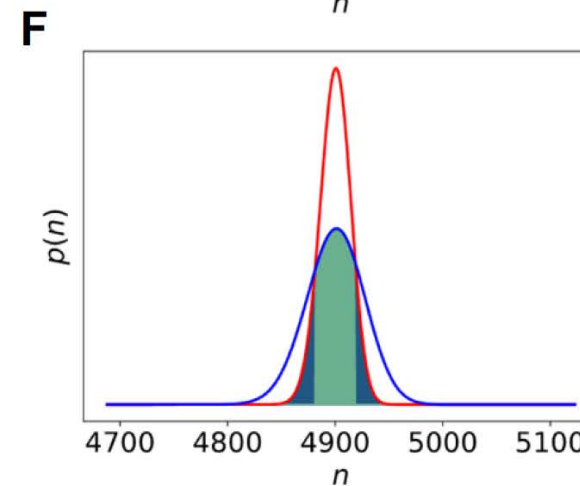
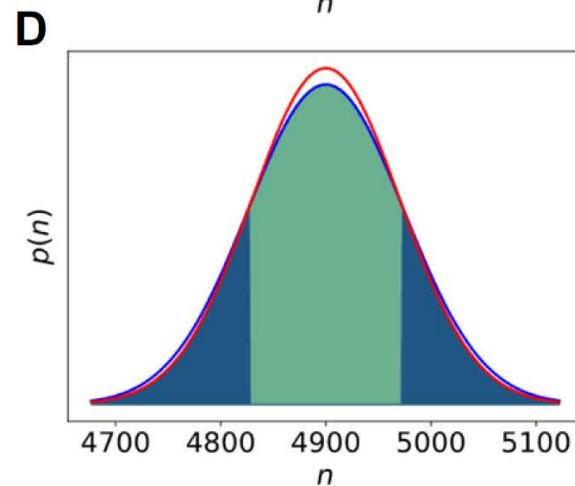
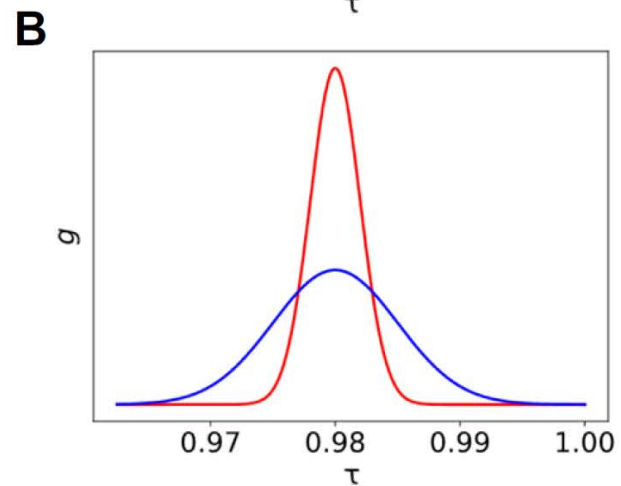
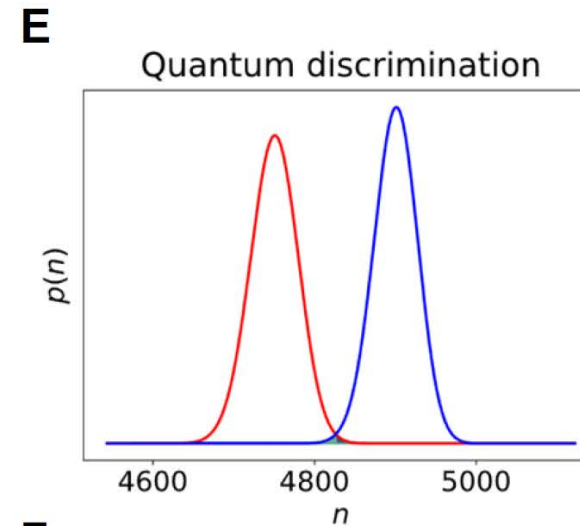
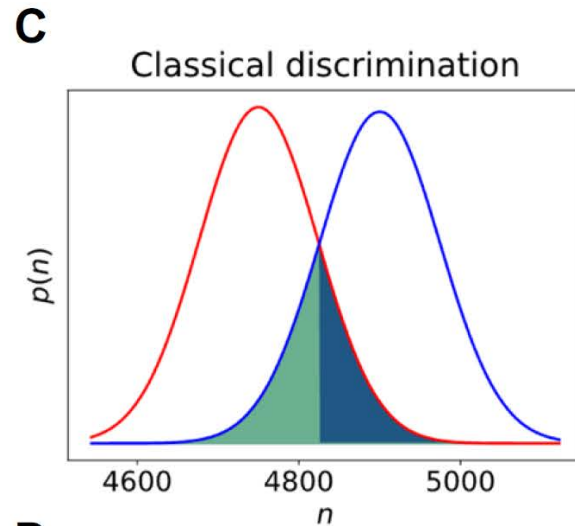
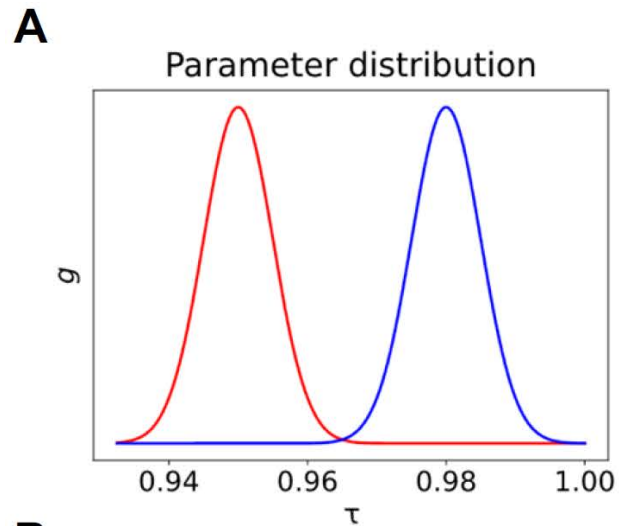


QUANTUM
TECHNOLOGIES

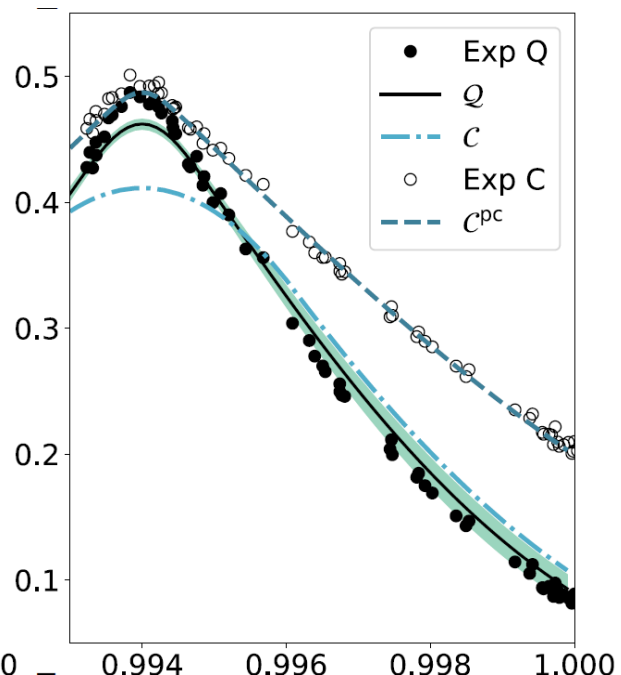
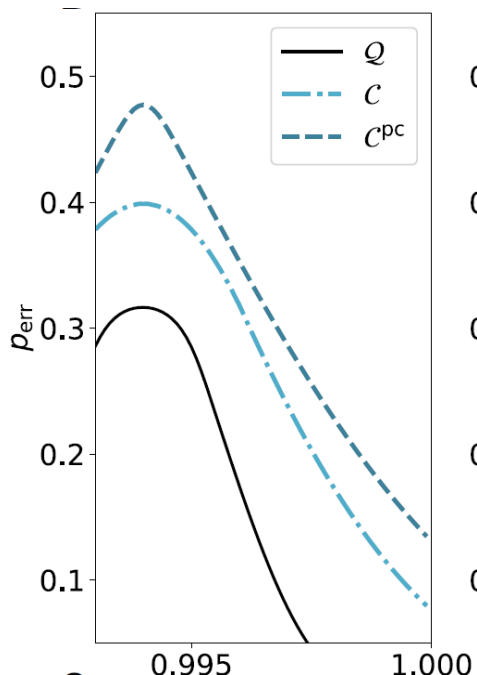
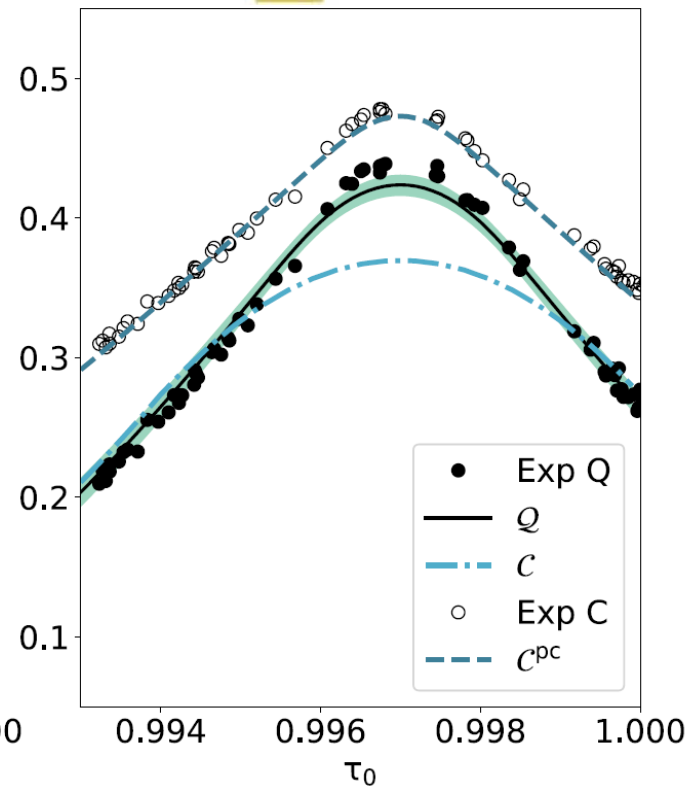
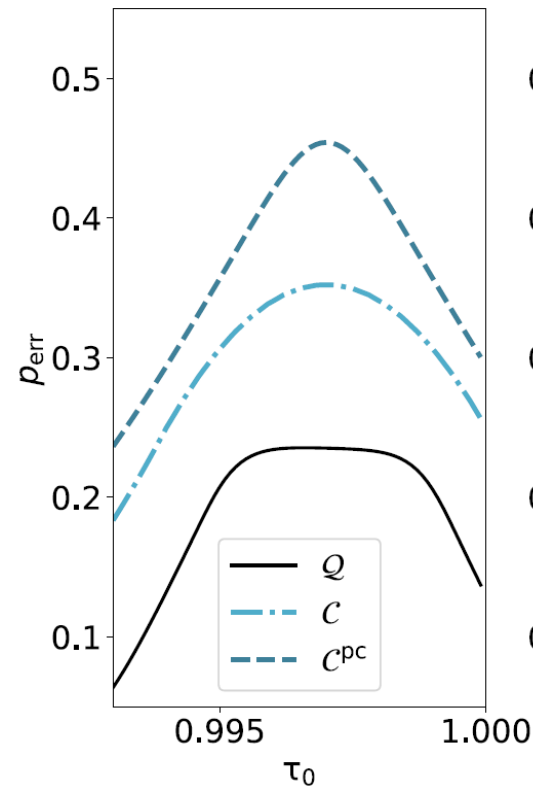
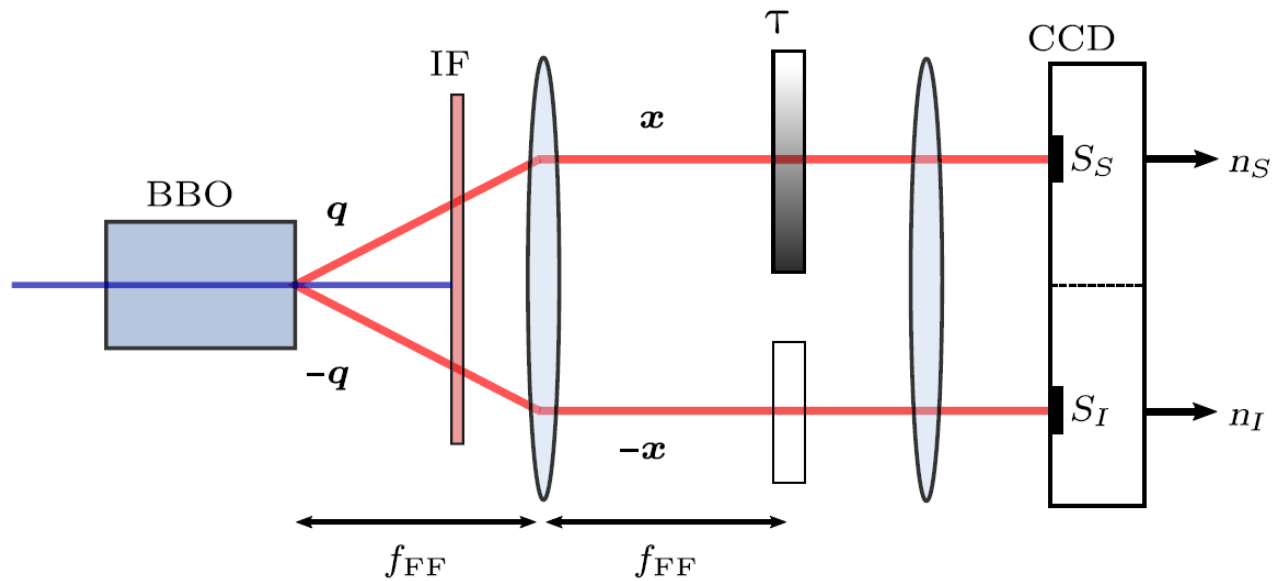
Ortolano et al., Sci. Adv.7, eabm3093 (2021)
Ortolano et al., Sci. Adv.7, eabc7796 (2021)



Quantum Conformance Test (Reading)



Quantum Conformance Test (Reading)



QUANTUM
TECHNOLOGIES

Ortolano et al., Sci. Adv.7, eabm3093 (2021)
Ortolano et al., Sci. Adv.7, eabc7796 (2021)



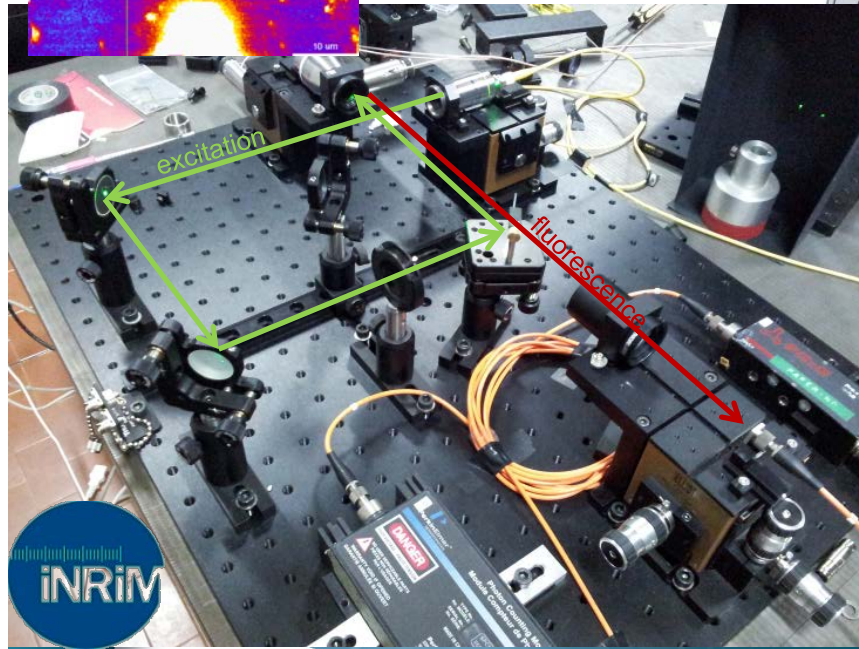
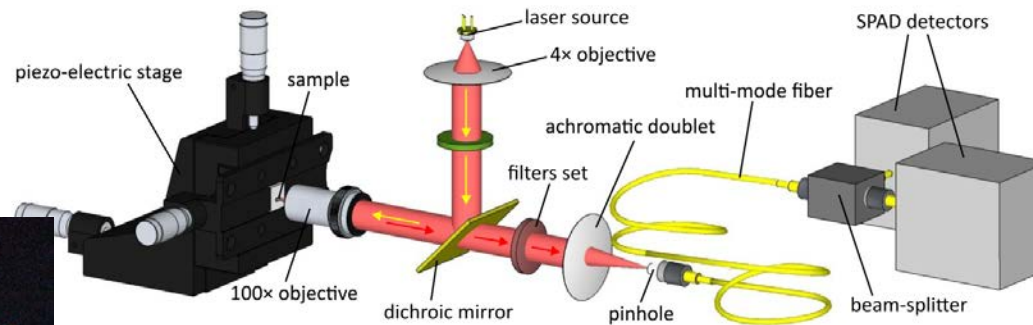
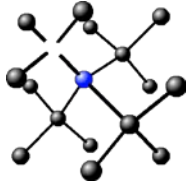
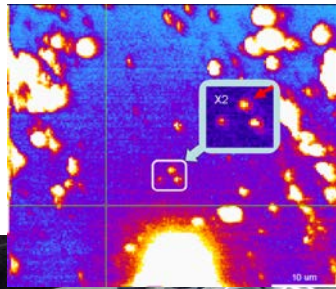
Color centers in diamond

5.5 eV energy gap can host several defects with optical transitions

Defects emitting in the visible spectrum: **color centers**

Point defects: individual optical transitions → single-photon emission

Operation at **room temperature**; **stable** (no photobleaching) **fluorescence**



SP-sensitive Confocal-Microsc.

- Off-resonant excitation: (Solid state diode lasers)
- Fibre Detection: coupled APD Perkin Elmer SPCM-AQR
- Air and oil objectives (NA = 0.9 and 1.3 resp.)



QUANTUM
TECHNOLOGIES

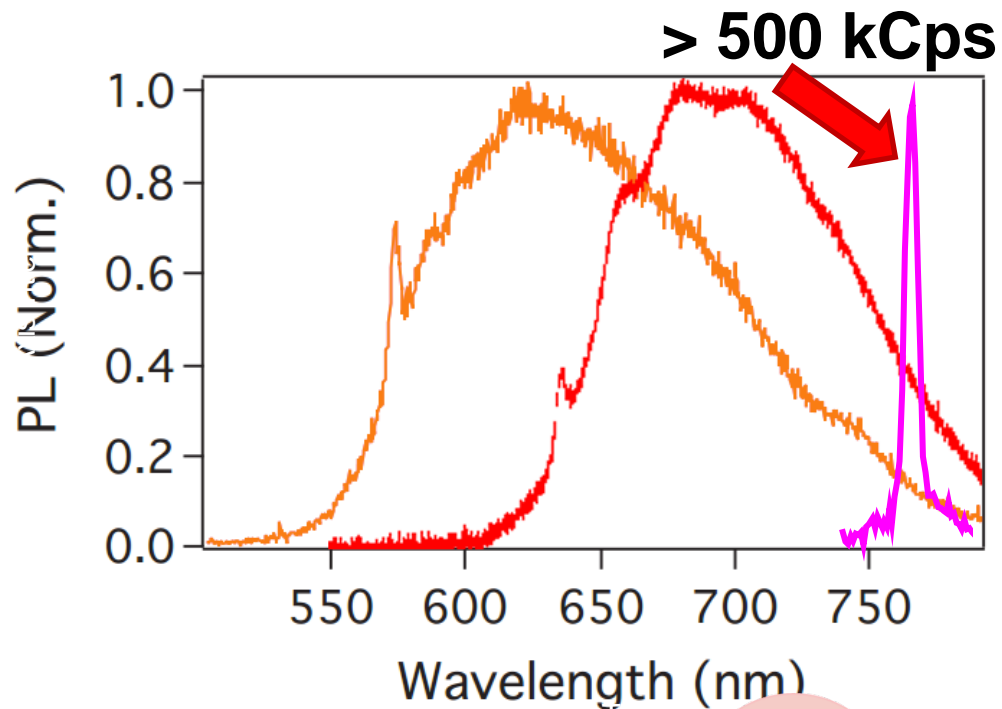
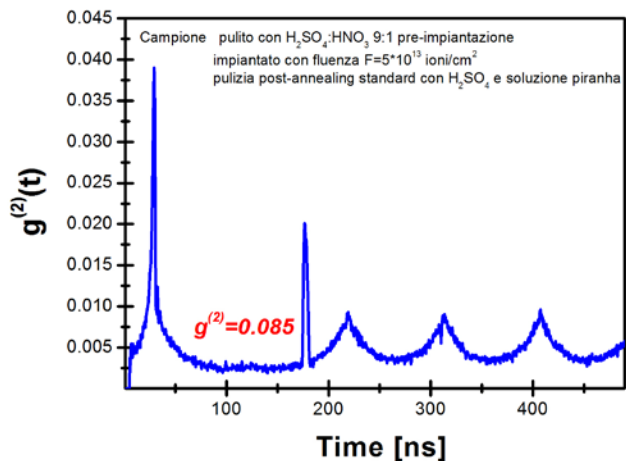
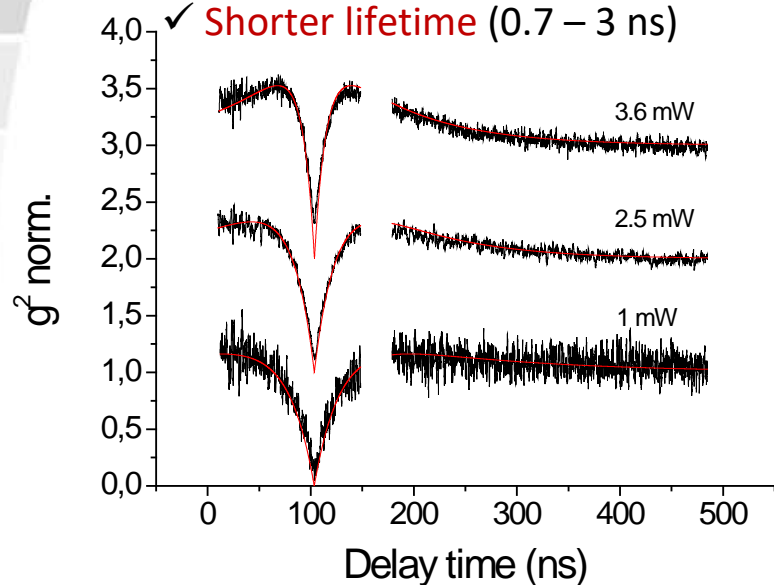


Color-centers as SPSs

Non-NV colour centres vs NV centers

✓ **Narrow emission** (< 5 nm, upper limit)

✓ **Shorter lifetime** (0.7 – 3 ns)

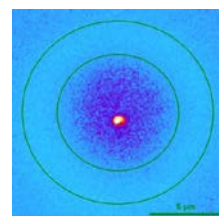
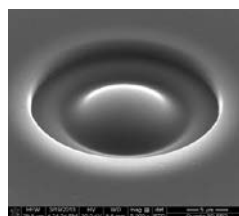
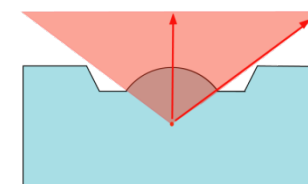
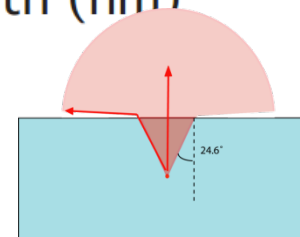


N-V: Metrologia **49**, S156 (2012)
Native NIR: NJP **16**, 053005 (2014)
Sn: ACS photonics **4**, 2580 (2017)
He: App.Phys.Lett. **111**, 111105 (2017)
Pb: ACS Photonics **5**, 4864 (2018)
N-V: P.R.App. **10**, 014024 (2018)
F: Sci.Rep. **10**, 1 (2020)
Pb: NJP **23**, 063032 (2021)
Mg: arxiv.org/abs/2206.08670 (2022)



QUANTUM TECHNOLOGIES

High diamond refractive index implies small limit angle for total internal reflection -> small amount of light collected



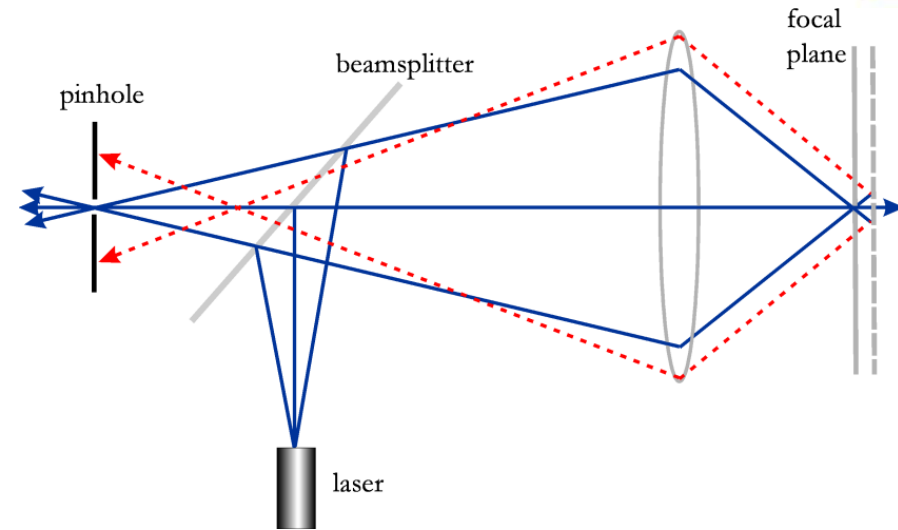
Solid immersion lens FIB (30 keV Ga⁺ FIB)
 5x collection increase

IJQI **12**, 1560011 (2014)



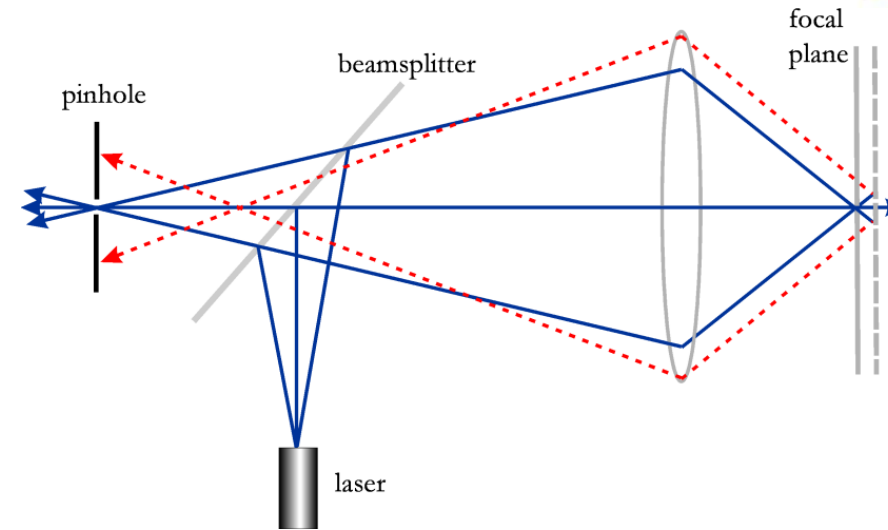
Confocal microscope

Confocal microscopy: imaging technique able to increase optical resolution and contrast of a micrograph by using **point illumination** and a **spatial pinhole** to eliminate out-of-focus light in specimens that are thicker than the focal plane. It enables the reconstruction of **3D** structures from the obtained images.

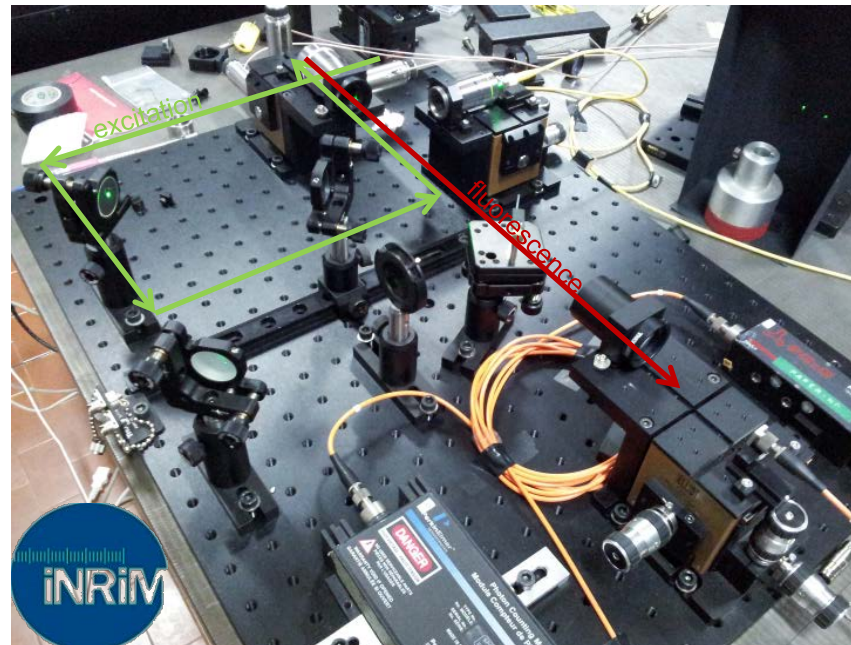


Confocal microscope

Confocal microscopy: imaging technique able to increase optical resolution and contrast of a micrograph by using **point illumination** and a **spatial pinhole** to eliminate out-of-focus light in specimens that are thicker than the focal plane. It enables the reconstruction of **3D** structures from the obtained images.



Single-photon confocal microscope



Abbe diffraction limit

The observation of sub-wavelength structures with microscopes is difficult because of the **Abbe diffraction limit**.

The maximum obtainable imaging resolution in classical far-field microscopy is

$$d = \frac{0.61 \lambda}{NA}$$

Beating the Abbe diffraction limit

- **Near-field microscopy:** plasmonic nanoantennas, nanosized tip ...
- **Far-field microscopy:**
 - **Optical patterning + Nonlinear response** (e.g. STED, SIM, ...)
 - **Single molecule imaging by photoactivation or photoswitching** (e.g. GSD, STORM, PALM, ...)



Abbe diffraction limit

The o
becau
The m



2014 Nobel Prize in Chemistry

The Nobel Prize in Chemistry 2014 was awarded jointly to Eric Betzig, Stefan W. Hell and William E. Moerner "for the development of super-resolved fluorescence microscopy".

Beati

- Near
- Far-fi
- C
- S
- G

s with microscopes is difficult

in classical far-field microscopy is

$$\lambda$$

mas, nanosized tip ...

(e.g. STED, SIM, ...)

ion or photoswitching (e.g.



QUANTUM TECHNOLOGIES

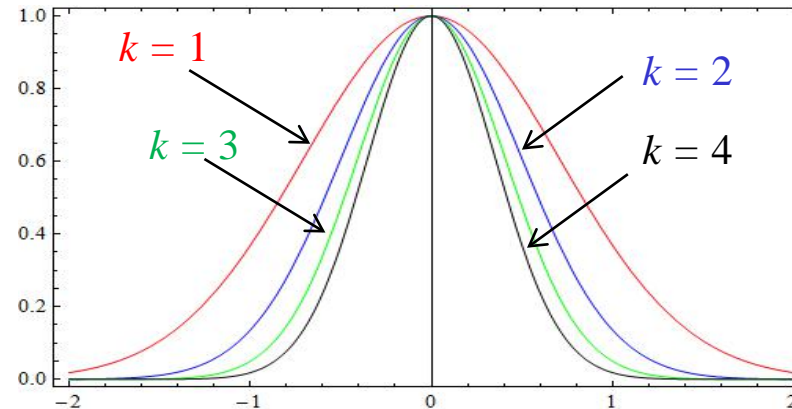


Beating the Abbe diffraction limit with SPSs

$\mathcal{P}(x)$ is essentially the PSF generated by the point-size SPS
(Probability of detecting a photon at the image position x from a single-photon source)

Reducing the size of PSF: $[\mathcal{P}(x)]^k$

$$\text{FWHM}^{(k)} \sim \frac{\text{FWHM}^{(1)}}{\sqrt{k}}$$

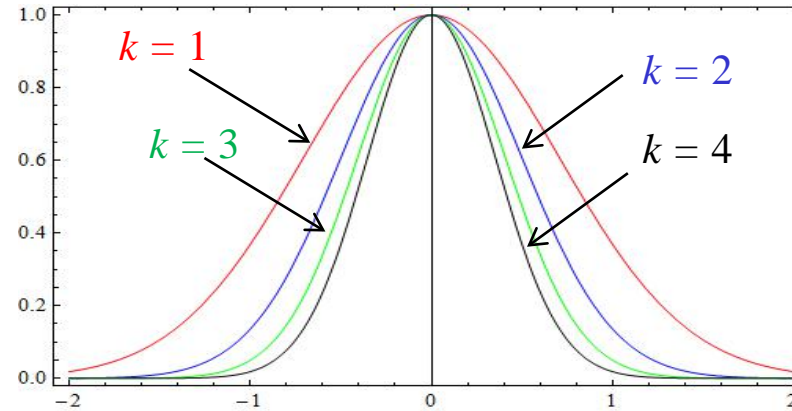


Beating the Abbe diffraction limit with SPSs

$\mathcal{P}(x)$ is essentially the PSF generated by the point-size SPS
 (Probability of detecting a photon at the image position x from a single-photon source)

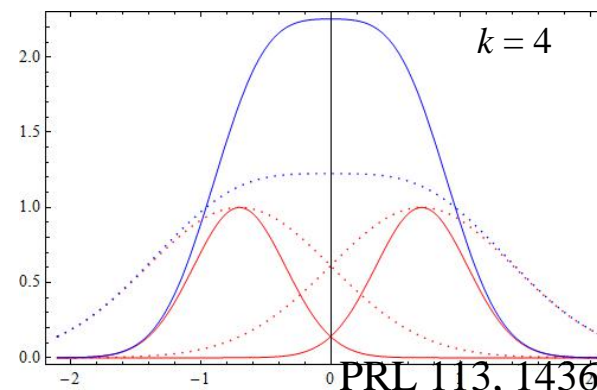
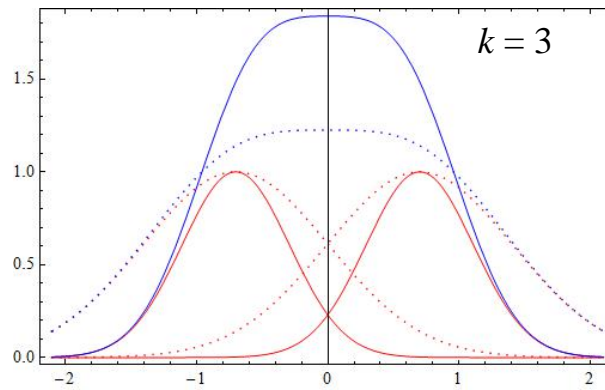
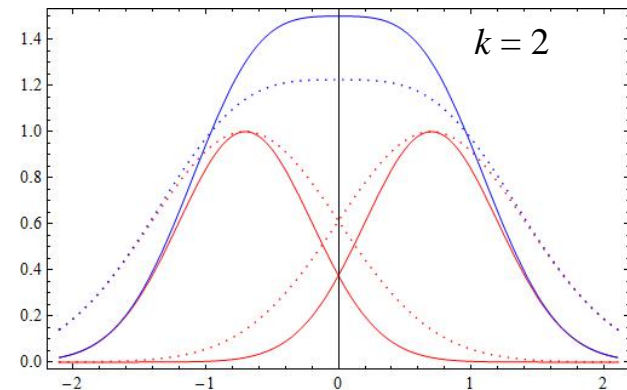
Reducing the size of PSF: $[\mathcal{P}(x)]^k$

$$\text{FWHM}^{(k)} \sim \frac{\text{FWHM}^{(1)}}{\sqrt{k}}$$



The fluorescence signal from n SPS at the position x : $S(x) \propto \sum_{\alpha=1}^n \mathcal{P}_{\alpha}(x)$

$$S^k(x)$$



PRL 113, 143602 (2014)



Beating the Abbe diffraction limit with SPSs

To improve the resolution:

$$S^k(x)$$

$$S(x) \propto \sum_{\alpha=1}^n \mathcal{P}_{\alpha}(x)$$



Beating the Abbe diffraction limit with SPSs

To improve the resolution:

~~$S^k(x)$~~

$$S(x) \propto \sum_{\alpha=1}^n \mathcal{P}_{\alpha}(x)$$



Beating the Abbe diffraction limit with SPSs

To improve the resolution:

$$\cancel{S^k(x)}$$

$$S(x) \propto \sum_{\alpha=1}^n \mathcal{P}_{\alpha}(x)$$

$$S^k(x) \propto \sum_{\alpha=1}^n [\mathcal{P}_{\alpha}(x)]^k + c.p.$$



$$\sum_{\alpha=1}^n [\mathcal{P}_{\alpha}(x)]^k$$



QUANTUM
TECHNOLOGIES



Beating the Abbe diffraction limit with SPSs

To improve the resolution:

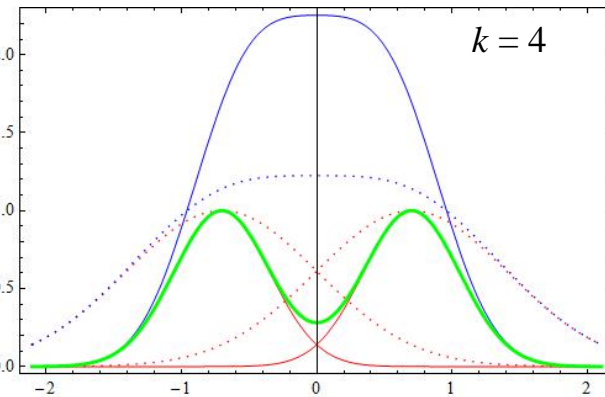
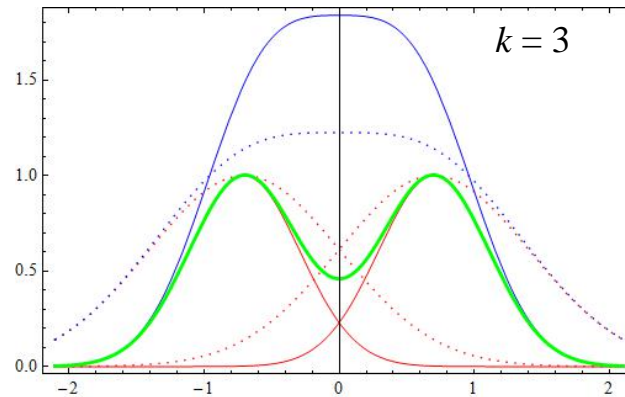
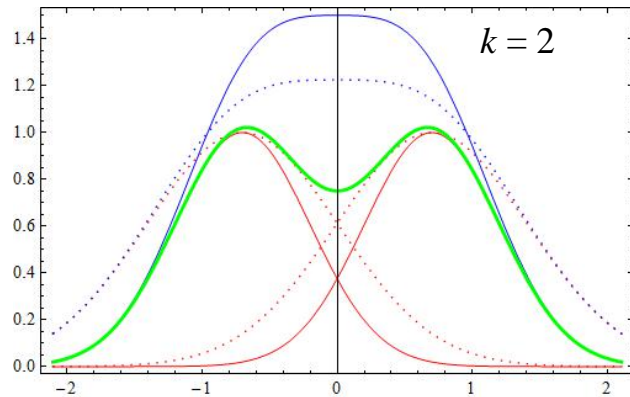
$$\cancel{S^k(x)}$$

$$S(x) \propto \sum_{\alpha=1}^n \mathcal{P}_{\alpha}(x)$$

$$S^k(x) \propto \sum_{\alpha=1}^n [\mathcal{P}_{\alpha}(x)]^k + \text{c.p.}$$



$$\sum_{\alpha=1}^n [\mathcal{P}_{\alpha}(x)]^k$$



QUANTUM TECHNOLOGIES



Beating the Abbe diffraction limit with SPSs

MODEL

To obtain the **resolution enhancement**:

$$\sum_{\alpha=1}^n [\mathcal{P}_{\alpha}(x)]^k$$

We exploit the Glauber's autocorrelation functions, e.g.

$$k=2 \quad \sum_{\alpha=1}^n [\mathcal{P}_{\alpha}(x)]^2 = \langle \hat{N} \rangle^2 [1 - g^{(2)}]$$

$$k=3 \quad \sum_{\alpha=1}^n [\mathcal{P}_{\alpha}(x)]^3 = \langle \hat{N} \rangle^3 [1 - \frac{3}{2}g^{(2)} + \frac{1}{2}g^{(3)}]$$

$$k=4 \quad \sum_{\alpha=1}^n [\mathcal{P}_{\alpha}(x)]^4 = \langle \hat{N} \rangle^4 \{1 - 2g^{(2)} + \frac{1}{2}[g^{(2)}]^2 + \frac{2}{3}g^{(3)} - \frac{1}{6}g^{(4)}\}$$

$$k=5 \quad \sum_{\alpha=1}^n [\mathcal{P}_{\alpha}(x)]^5 = \langle \hat{N} \rangle^5 \{1 - \frac{5}{2}g^{(2)} + \frac{5}{4}[g^{(2)}]^2 + \frac{5}{6}g^{(3)} - \frac{5}{12}g^{(2)}g^{(3)} - \frac{5}{24}g^{(4)} + \frac{1}{24}g^{(5)}\}$$

...

PRL 113, 143602 (2014)

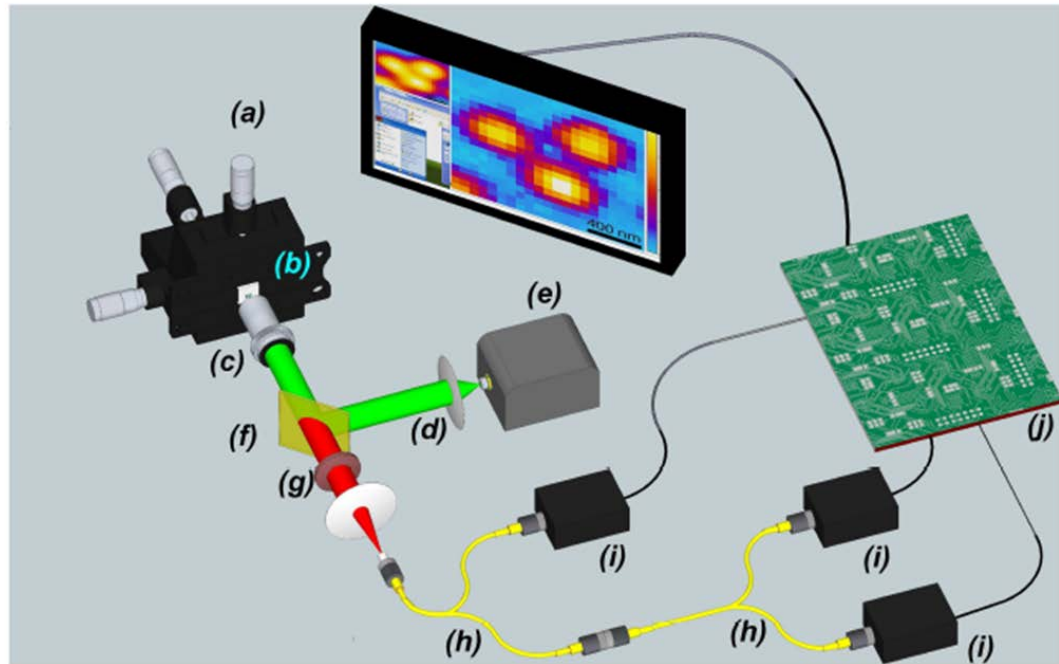


QUANTUM
TECHNOLOGIES

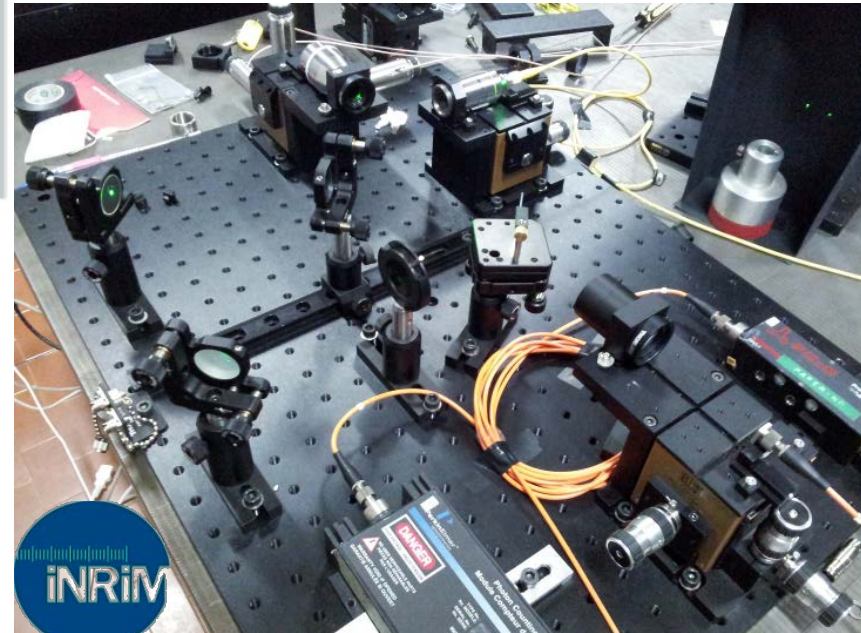


Beating the Abbe diffraction limit with SPCs

EXPERIMENTAL SETUP & RESULTS



- Excitation: @ 532 nm (Solid state diode laser)
- XYZ closed-loop piezo stage
- Detection $\lambda > 570$ nm
- Fibre coupled SPCMs in a **Detector Tree** configuration.
- 100X oil objective (NA = 1.3)



PRL 113, 143602 (2014)



QUANTUM TECHNOLOGIES



Beating the Abbe diffraction limit with SPSs

EXPERIMENTAL SETUP & RESULTS

elementsix™

electronic-grade Polycrystalline diamond

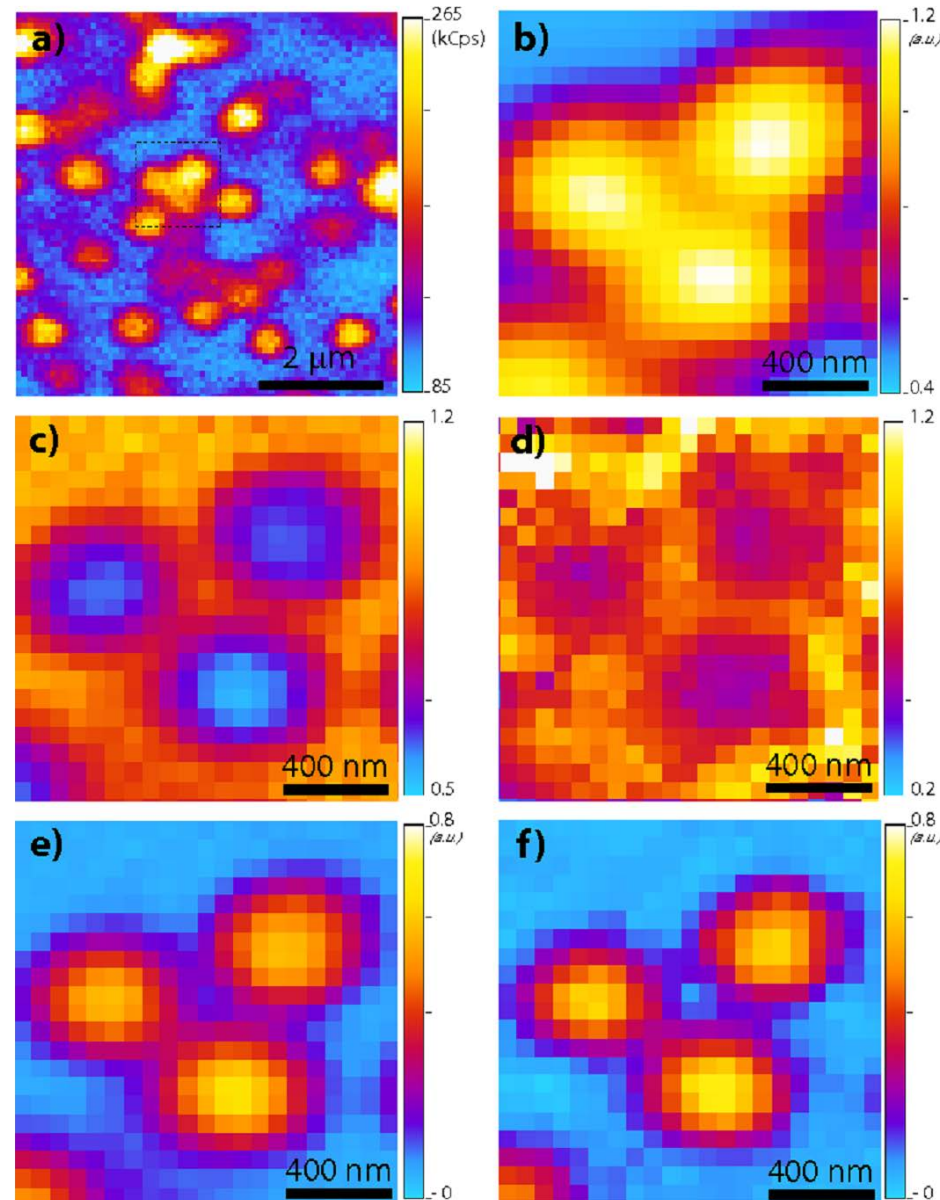
(a)&(b) typical photoluminescence maps of NV centers

(c) $g^{(2)}$ map

(d) $g^{(3)}$ map

(e) Super-resolved map ($k = 2$)

(f) Super-resolved map ($k = 3$)



PRL 113, 143602 (2014)



QUANTUM TECHNOLOGIES



Beating the Abbe diffraction limit with SPSs

EXPERIMENTAL SETUP & RESULTS

elementsix.
electronic

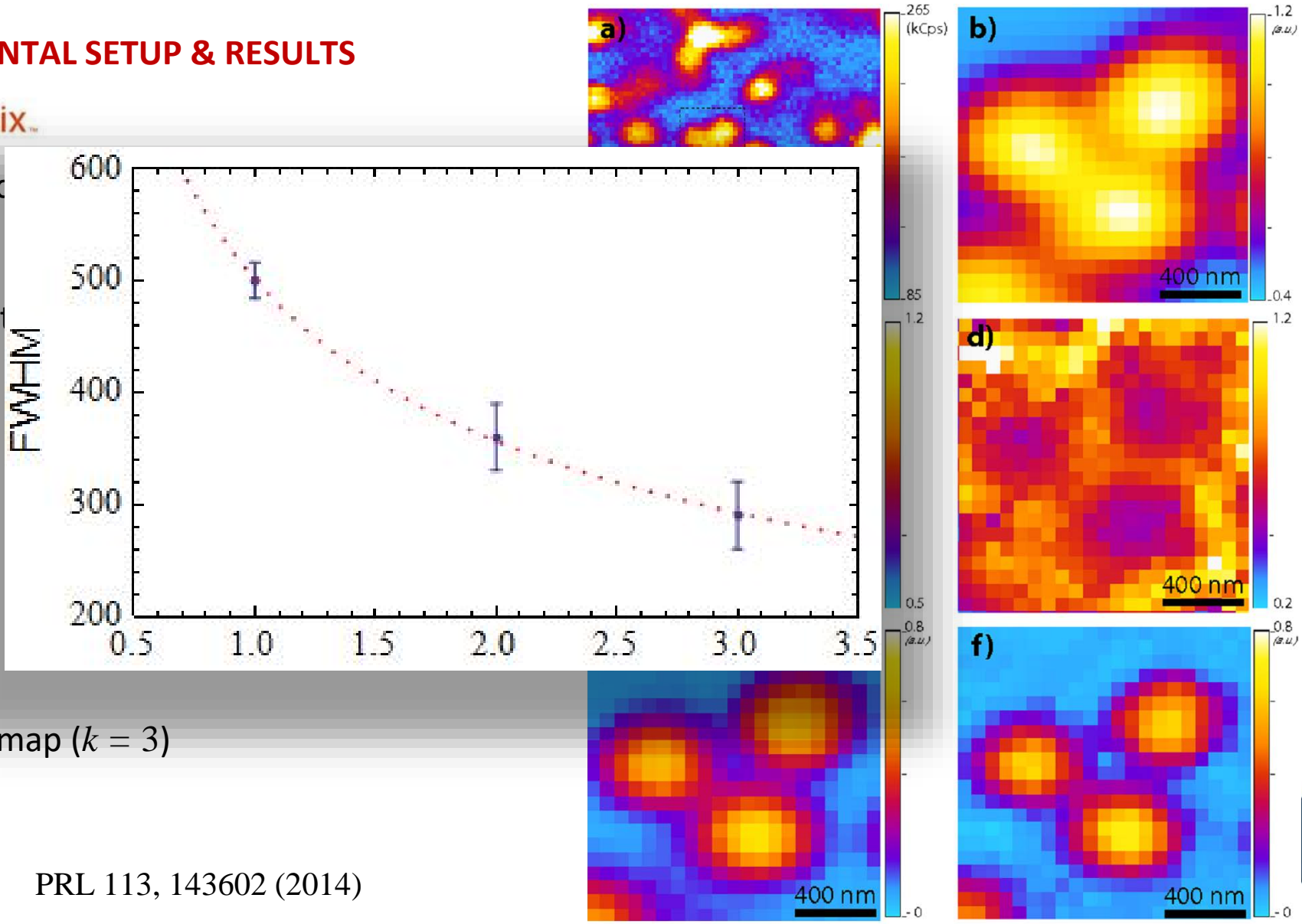
(a)&(b) typical photonic centers

(c) $g^{(2)}$ map

(d) $g^{(3)}$ map

(e) Super-resolved

(f) Super-resolved map ($k = 3$)



PRL 113, 143602 (2014)



QUANTUM TECHNOLOGIES



Beating the Abbe diffraction limit with SPSs

EXPERIMENTAL SETUP & RESULTS

(a) photoluminescence maps of NV centers

(b) $g^{(2)}$ map

(c) Super-resolved map ($k = 2$)

$$\langle \hat{N} \rangle^2 [1 - g^{(2)}]$$

$$g^{(3)} = 0$$

(d) Super-resolved map ($k = 3$)

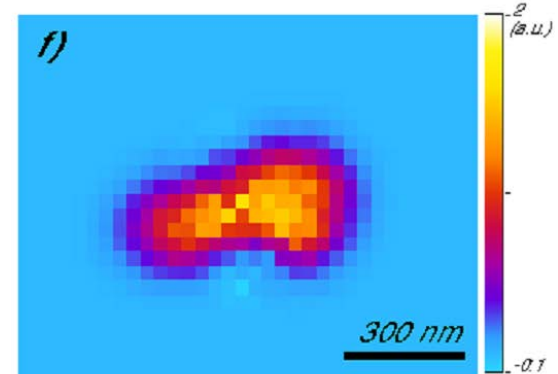
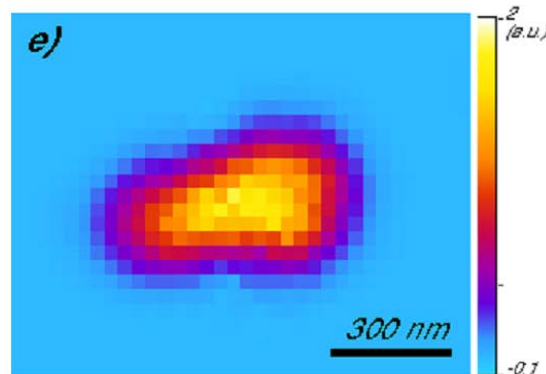
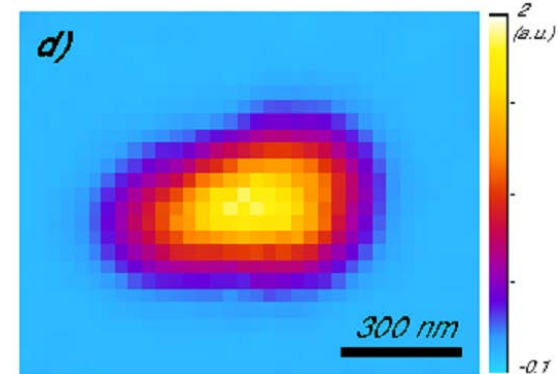
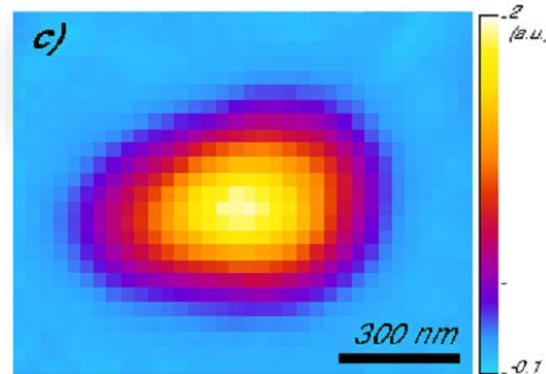
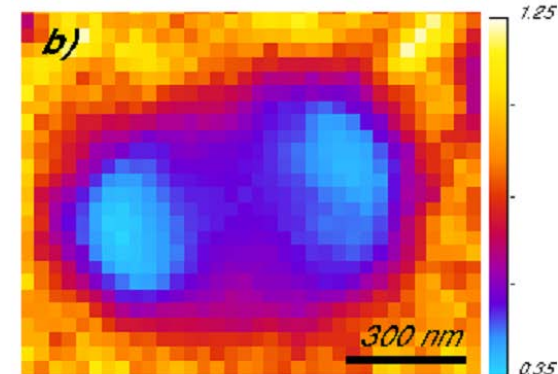
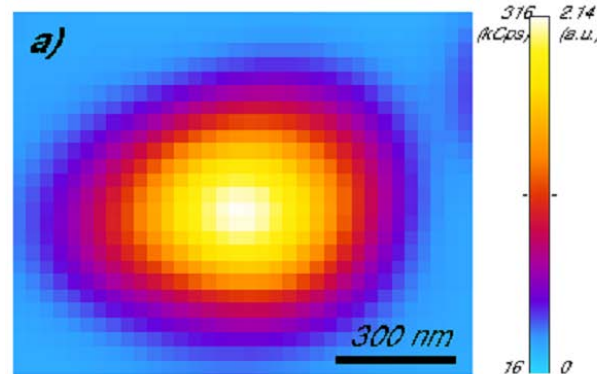
$$\langle \hat{N} \rangle^3 [1 - \frac{3}{2}g^{(2)} + \frac{1}{2}g^{(3)}]$$

(e) Super-resolved map ($k = 4$)

$$\langle \hat{N} \rangle^4 \{1 - 2g^{(2)} + \frac{1}{2}[g^{(2)}]^2 + \frac{8}{3}g^{(3)} - \frac{1}{6}g^{(4)}\}$$

(f) Super-resolved map ($k = 5$)

$$\langle \hat{N} \rangle^5 \{1 - \frac{5}{2}g^{(2)} + \frac{5}{4}[g^{(2)}]^2 + \frac{5}{6}g^{(3)} - \frac{5}{12}g^{(4)} + \frac{5}{24}g^{(5)}\}$$



QUANTUM TECHNOLOGIES



Beating the Abbe diffraction limit with SPSs

EXPERIMENTAL SETUP & RESULTS

(a) photoluminescence maps of NV centers

(b) $g^{(2)}$ map

(c) Super-resolved map ($k = 2$)

$$\langle \hat{N} \rangle^2 [1 - g^{(2)}]$$

$$g^{(3)} = 0$$

(d) Super-resolved map ($k = 3$)

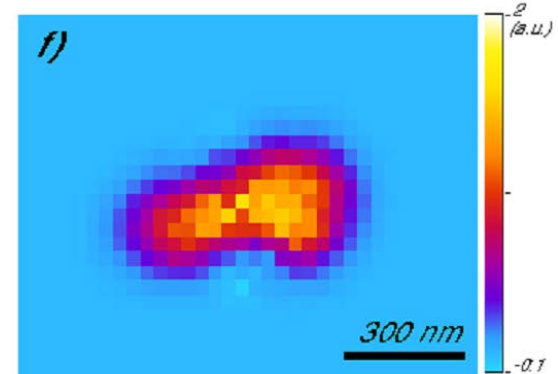
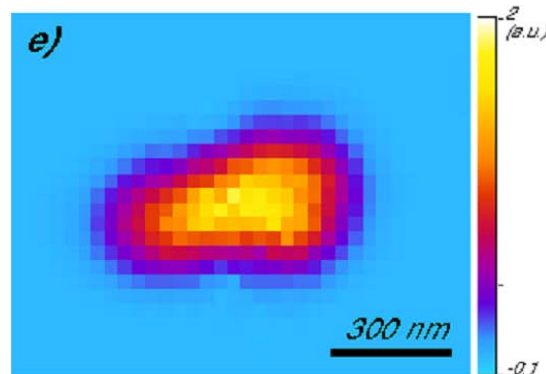
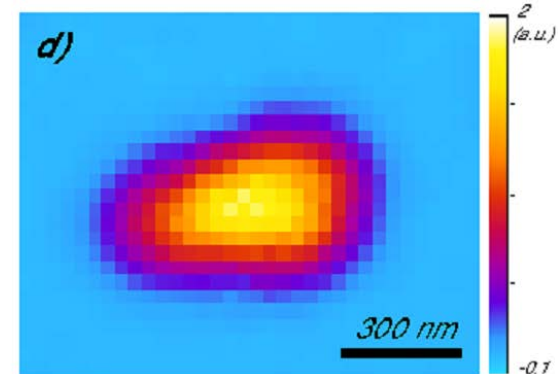
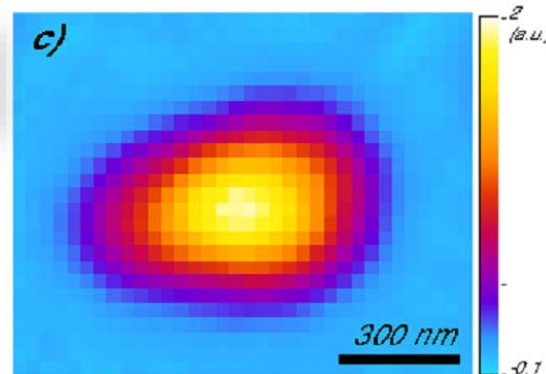
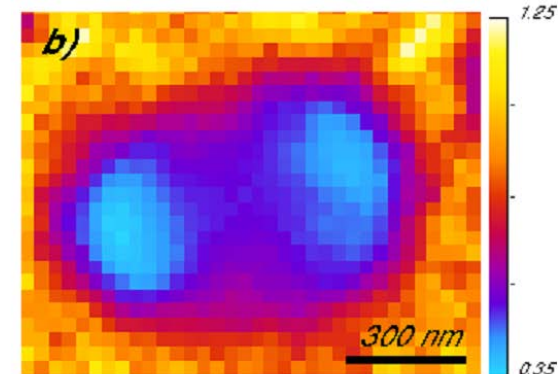
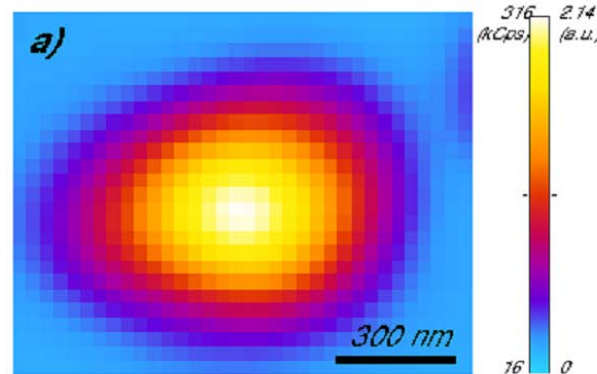
$$\langle \hat{N} \rangle^3 [1 - \frac{3}{2}g^{(2)} + \frac{1}{2}g^{(3)}]$$

(e) Super-resolved map ($k = 4$)

$$\langle \hat{N} \rangle^4 \{1 - 2g^{(2)} + \frac{1}{2}[g^{(2)}]^2 + \frac{2}{3}g^{(3)} - \frac{1}{6}g^{(4)}\}$$

(f) Super-resolved map ($k = 5$)

$$\langle \hat{N} \rangle^5 \{1 - \frac{5}{2}g^{(2)} + \frac{5}{4}[g^{(2)}]^2 + \frac{5}{6}g^{(3)} - \frac{5}{12}g^{(4)} + \frac{5}{24}g^{(5)}\}$$



QUANTUM TECHNOLOGIES



Beating the Abbe diffraction limit with SPSs

EXPERIMENTAL SETUP & RESULTS

(a) photoluminescence maps of NV centers

(b) $g^{(2)}$ map

(c) Super-resolved map ($k = 2$)

$$\langle \hat{N} \rangle^2 [1 - g^{(2)}]$$

$$g^{(3)} = 0$$

(d) Super-resolved map ($k = 3$)

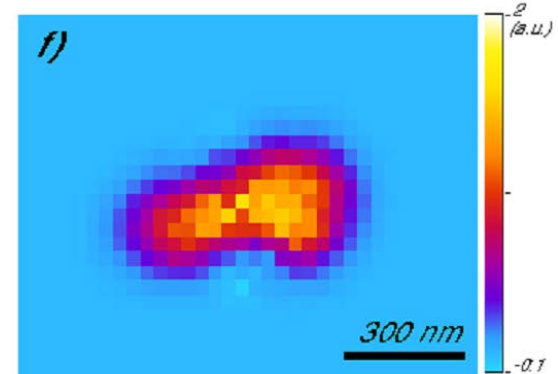
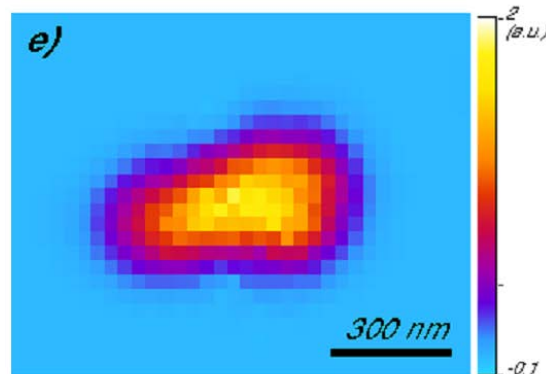
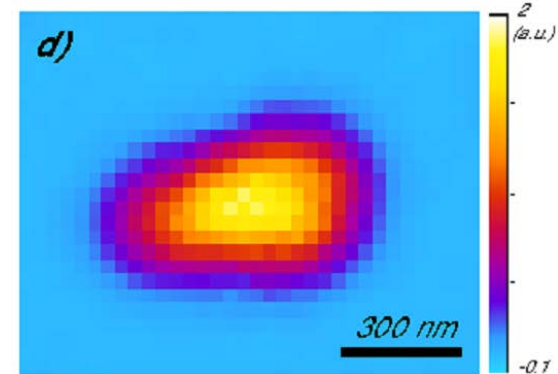
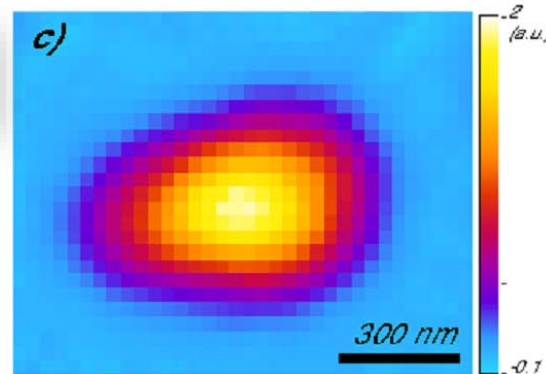
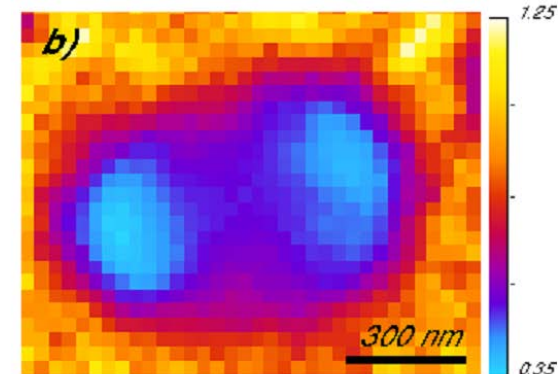
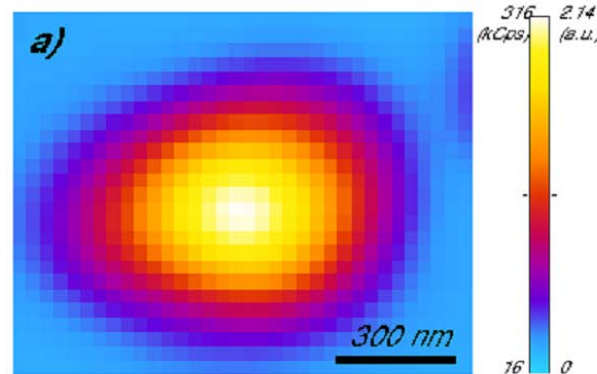
$$\langle \hat{N} \rangle^3 [1 - \frac{3}{2}g^{(2)} + \frac{1}{2}g^{(3)}]$$

(e) Super-resolved map ($k = 4$)

$$\langle \hat{N} \rangle^4 \{1 - 2g^{(2)} + \frac{1}{2}[g^{(2)}]^2 + \frac{8}{3}g^{(3)} - \frac{1}{6}g^{(4)}\}$$

(f) Super-resolved map ($k = 5$)

$$\langle \hat{N} \rangle^5 \{1 - \frac{5}{2}g^{(2)} + \frac{5}{4}[g^{(2)}]^2 + \frac{5}{6}g^{(3)} - \frac{5}{12}g^{(2)}g^{(3)} - \frac{5}{24}g^{(4)} + \frac{1}{24}g^{(5)}\}$$



QUANTUM TECHNOLOGIES



Traditional "sharp" measurement in QM

Standard "sharp" measurement:

$$\hat{A} = \sum_n \lambda_n \hat{\Pi}_n \quad \hat{\Pi}_n = |\psi_n\rangle\langle\psi_n| \quad \text{Tr}[\hat{A}\hat{\rho}] = \sum_n \lambda_n \text{Tr}[\hat{\Pi}_n\hat{\rho}]$$

Single projective measurement:

$$\hat{\rho} \xrightarrow{\hat{\Pi}_k} |\psi_k\rangle \quad \text{Prob}(\psi_k|\rho) = \text{Tr}[\hat{\Pi}_k\hat{\rho}]$$

Joint/sequential projective measurements:

$$\hat{\rho} \xrightarrow{\hat{\Pi}_k} |\psi_k\rangle \xrightarrow{\hat{\Pi}_n} |\psi_n\rangle \quad \text{Tr}[\hat{\Pi}_n \hat{\Pi}_k \hat{\rho}] \dots ?$$

Wave function collapse



Non-commuting
observables can't be
simultaneously measured!

$$\text{Tr} \left[\hat{\Pi}_n \left(\hat{\Pi}_k \hat{\rho} \hat{\Pi}_k \right) \right] = \text{Prob}(\psi_n|\psi_k) \text{Prob}(\psi_k|\rho)$$

Weak measurements

Weak measurements [Aharonov et al., PRL 60 (1988)]: little information is extracted from a single measurement event, but the state does NOT collapse.

Weak value: $\langle \hat{A} \rangle_w = \frac{\langle \psi_f | \hat{A} | \psi_i \rangle}{\langle \psi_f | \psi_i \rangle}$

Pre-selected state: $|\psi_i\rangle$
 Post-selected state: $|\psi_f\rangle$

Von Neumann coupling between an observable \hat{A} and a pointer observable \hat{P} :

$$\hat{U} = \exp(-ig\hat{A} \otimes \hat{P})$$

Projective measurement (post-selection on $|\psi_f\rangle$): $\hat{\Pi}_f = |\psi_f\rangle\langle\psi_f|$

$$|\Psi_{out}\rangle = \hat{\Pi}_f \hat{U} |\Psi_{in}\rangle = \hat{\Pi}_f \hat{U} |\psi_i\rangle \otimes |\phi_p\rangle$$

\hat{X} and \hat{P}
 canonically
 conjugated

Weak interaction approximation: \rightarrow

$$\langle \hat{X} \rangle = \frac{\langle \Psi_{out} | \hat{X} | \Psi_{out} \rangle}{\langle \psi_i | \hat{\Pi}_f | \psi_i \rangle} = g \operatorname{Re}[\langle \hat{A} \rangle_w]$$

Weak measurements

Some interesting properties:

$\langle \hat{A} \rangle_w$ is a complex number

$\text{Re}[\langle \hat{A} \rangle_w]$ is unbounded!

$$\langle \hat{A} \rangle_w = \frac{\langle \psi_f | \hat{A} | \psi_i \rangle}{\langle \psi_f | \psi_i \rangle}$$

$$\hat{U} = \exp(-ig\hat{A} \otimes \hat{P})$$

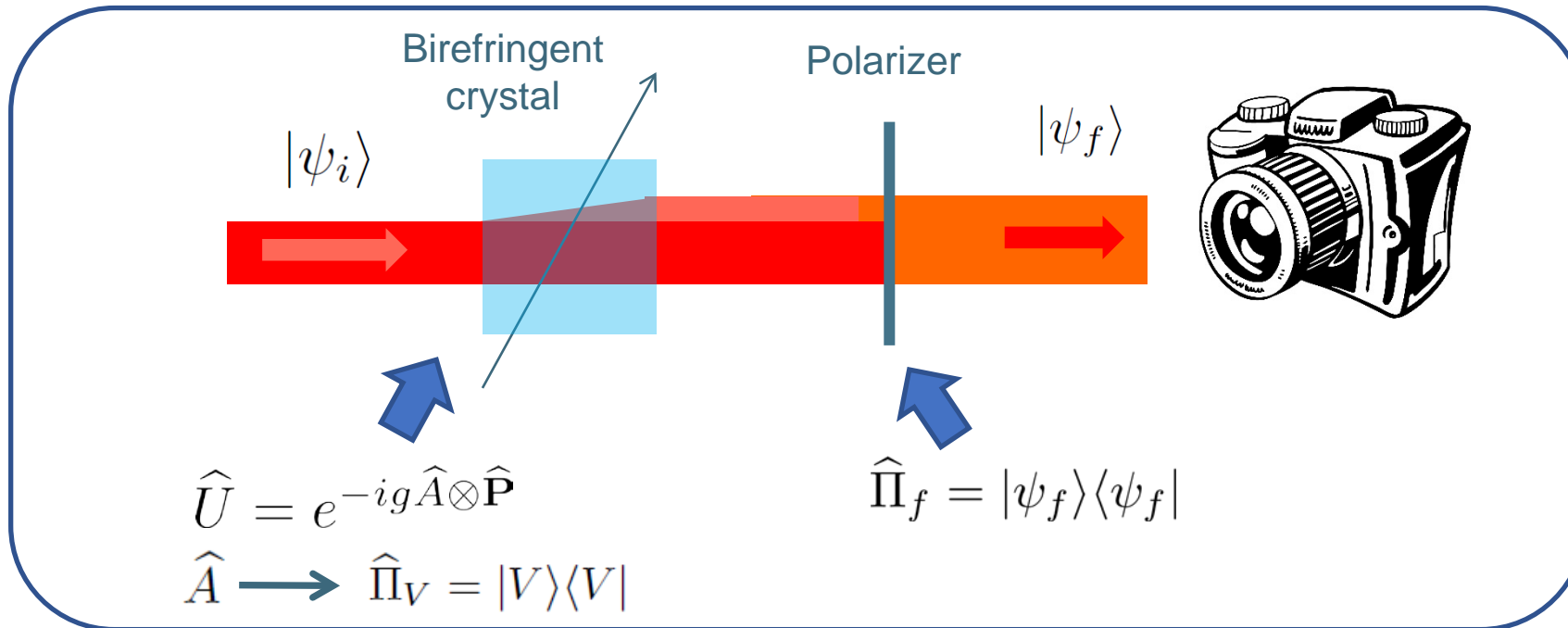
$$\hat{\Pi}_f = |\psi_f\rangle\langle\psi_f|$$

Interpretation of weak values:

- $\text{Re}[\langle \hat{A} \rangle_w]$ conditioned average in the limit of 0 disturbance [Dressel et al., PRL 104 (2010)]
- $\text{Im}[\langle \hat{A} \rangle_w]$ arising from disturbance related to the von Neumann coupling [Dressel and Jordan, PRA 85 (2012)]
- Expectation values as averages of weak values [Aharonov and Botero, PRA 72 (2005)]
$$\langle A \rangle_i = \sum_f |\langle \psi_i | \psi_f \rangle|^2 \langle \hat{A} \rangle_w$$
- POVMs can be realized as a sequence of weak values [Oreshkov and Brun, PRL 95 (2005)]

Weak measurements with photons

Initial state: $|\psi_i\rangle = \cos \theta_i |H\rangle + \sin \theta_i |V\rangle$ polarization component
 $|\Psi_{in}\rangle = |\psi_i\rangle \otimes |\phi_x\rangle \rightarrow |\phi_x\rangle = \frac{1}{\sqrt{\sigma}\sqrt{2\pi}} \int dx e^{-\frac{x^2}{4\sigma^2}} |x\rangle$ spatial (Gaussian) component



We measure the position observable \hat{X} , canonically conjugated to the transverse momentum \hat{P}

$$\langle \hat{X} \rangle = g \text{Re}[\langle \hat{\Pi}_V \rangle_w]$$

Joint and sequential weak measurements

Weak values «challenge one of the canonical dicta of QM: that non commuting observables cannot be simultaneously measured»

«the fact that one hardly disturbs the systems in making WM means that one can in principle *measure different variables in succession*» [Mitchison, Jozsa and Popescu, PRA 76 (2007)]

Joint weak measurement

Resch et al., PRL 92, 130402 (2004)

$$\hat{U} = \exp[-i(g_x \hat{A} \otimes \hat{P}_x + g_y \hat{B} \otimes \hat{P}_y)]$$

$$\langle \hat{X}\hat{Y} \rangle = \frac{1}{4} g_x g_y \text{Re} \left[\langle \hat{A}\hat{B} + \hat{B}\hat{A} \rangle_w + 2\langle \hat{A} \rangle_w^* \langle \hat{B} \rangle_w \right]$$

Sequential weak measurement

Mitchinson et al., PRA 76, 062105 (2007)

$$\hat{U}_y = \exp(-i g_y \hat{B} \otimes \hat{P}_y)$$



$$\hat{U}_x = \exp(-i g_x \hat{A} \otimes \hat{P}_x)$$

$$\langle \hat{X}\hat{Y} \rangle = \frac{1}{2} g_x g_y \text{Re} \left[\langle \hat{A}\hat{B} \rangle_w + \langle \hat{A} \rangle_w^* \langle \hat{B} \rangle_w \right]$$

Sequential weak measurements

$$\hat{A} \longrightarrow \hat{\Pi}_V = |V\rangle\langle V|$$

$$\hat{B} \longrightarrow \hat{\Pi}_\psi = |\psi\rangle\langle\psi|$$

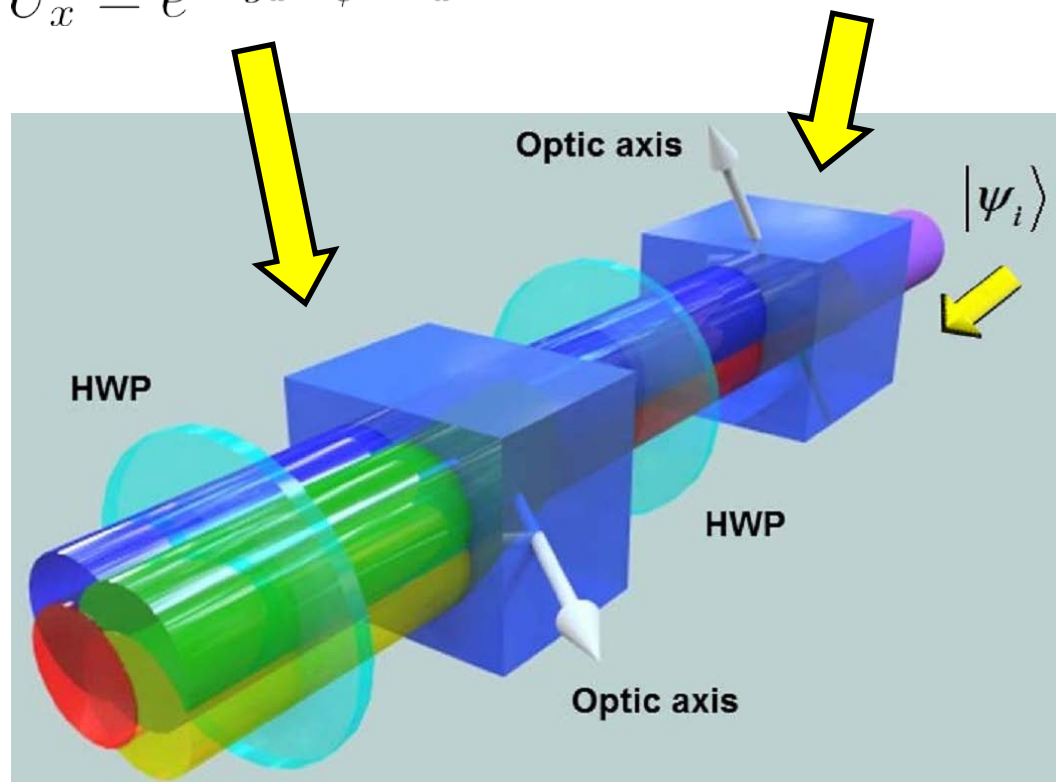
$$|\psi\rangle = \cos\theta|H\rangle + \sin\theta|V\rangle$$

Linearly polarized pre- and post-selection states

$$|\psi_i\rangle, |\psi_f\rangle$$

$$\left\{ \begin{array}{l} \langle \hat{X} \rangle = g_x \langle \hat{\Pi}_\psi \rangle_w \\ \langle \hat{Y} \rangle = g_y \langle \hat{\Pi}_V \rangle_w \\ \langle \hat{X}\hat{Y} \rangle = \frac{1}{2} g_x g_y \left(\langle \hat{\Pi}_\psi \hat{\Pi}_V \rangle_w + \langle \hat{\Pi}_\psi \rangle_w \langle \hat{\Pi}_V \rangle_w \right) \end{array} \right.$$

$$\hat{U}_x = e^{-ig_x \hat{\Pi}_\psi \otimes \hat{P}_x} \quad \hat{U}_y = e^{-ig_y \hat{\Pi}_V \otimes \hat{P}_y}$$



Sequential weak measurements



32x32

SPAD+TDC camera

Features

- Multi-modality: photon-counting, 2D imaging, 3D time-of-flight ranging, TCSPC (time-correlated single-photon counting)
- Image dimension: 32x32 (1024) pixels
- In-pixel counter: 6 bit (photon-counting)
- In-pixel TDC: 10 bit (photon-timing)
- Max frame rate: 100,000 fps (burst) and 10,000 fps (continuous)
- Timing resolution: 312 ps – 0.9 ns
- Full scale range: 320 ns – 0.92 μ s
- Hardware interface: USB 2.0
- Software interface: Matlab



Fig. 1: SPAD camera for 2D imaging, 3D ranging and TCSPC photon-counting.



POLITECNICO
MILANO 1863

F. Villa et al., CMOS imager with 1024 SPADs and TDCs 474 for single-photon timing and 3-D time-of-flight,
IEEE J. Sel. 475 Top. Quantum Electron. 20, 364 (2014).



QUANTUM
TECHNOLOGIES

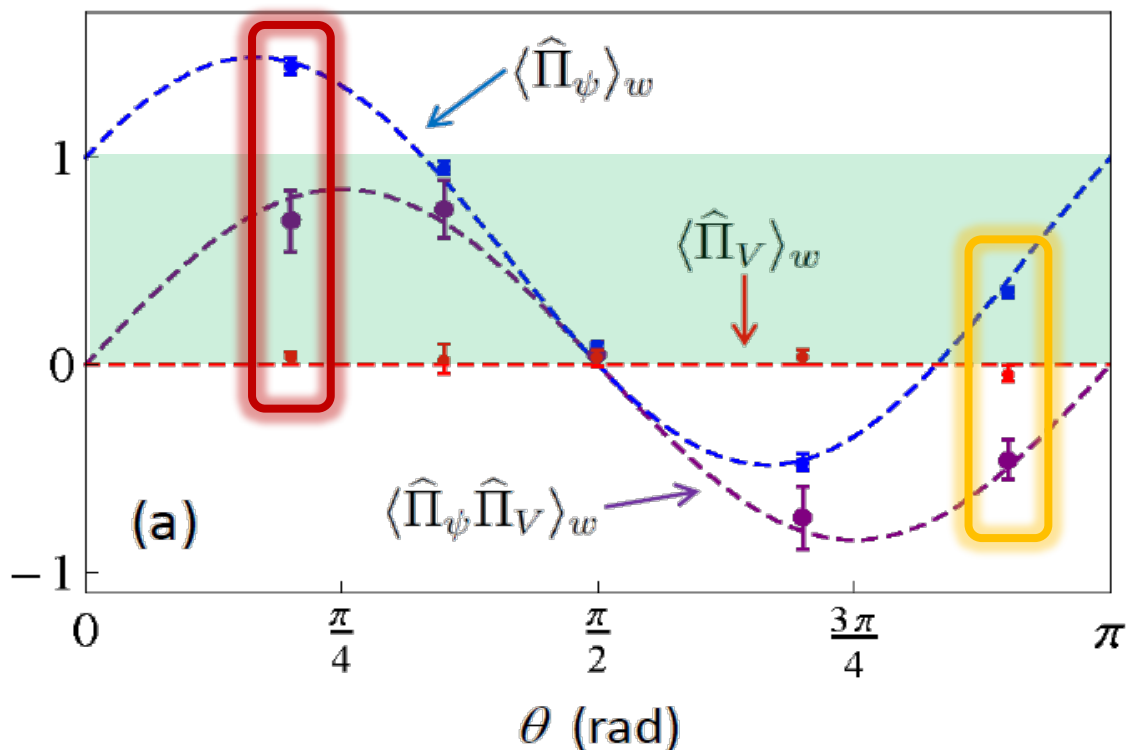


Sequential weak measurements

Measured weak values (data points) compared with the theoretical predictions (curves)

$$\hat{\Pi}_V = |V\rangle\langle V| \quad \hat{\Pi}_\psi = |\psi\rangle\langle\psi| \quad (|\psi\rangle = \cos\theta|H\rangle + \sin\theta|V\rangle)$$

$$|\psi_i\rangle = 0.588|H\rangle + 0.809|V\rangle \quad |\psi_f\rangle = |H\rangle$$



$$\langle \hat{\Pi}_V \rangle_w = 0.03(3)$$

$$\langle \hat{\Pi}_\psi \rangle_w = 1.44(4)$$

$$\langle \hat{\Pi}_\psi \hat{\Pi}_V \rangle_w = 0.69(15)$$

$$\langle \hat{\Pi}_V \rangle_w = -0.04(3)$$

$$\langle \hat{\Pi}_\psi \rangle_w = 0.35(4)$$

$$\langle \hat{\Pi}_\psi \hat{\Pi}_V \rangle_w = -0.46(10)$$



Sequential weak measurements

Measured weak values (data points) compared with the theoretical predictions (curves)

$$\hat{\Pi}_V = |V\rangle\langle V|$$

$$\hat{\Pi}_\psi = |\psi\rangle\langle\psi| \quad (|\psi\rangle = \cos\theta|H\rangle + \sin\theta|V\rangle)$$

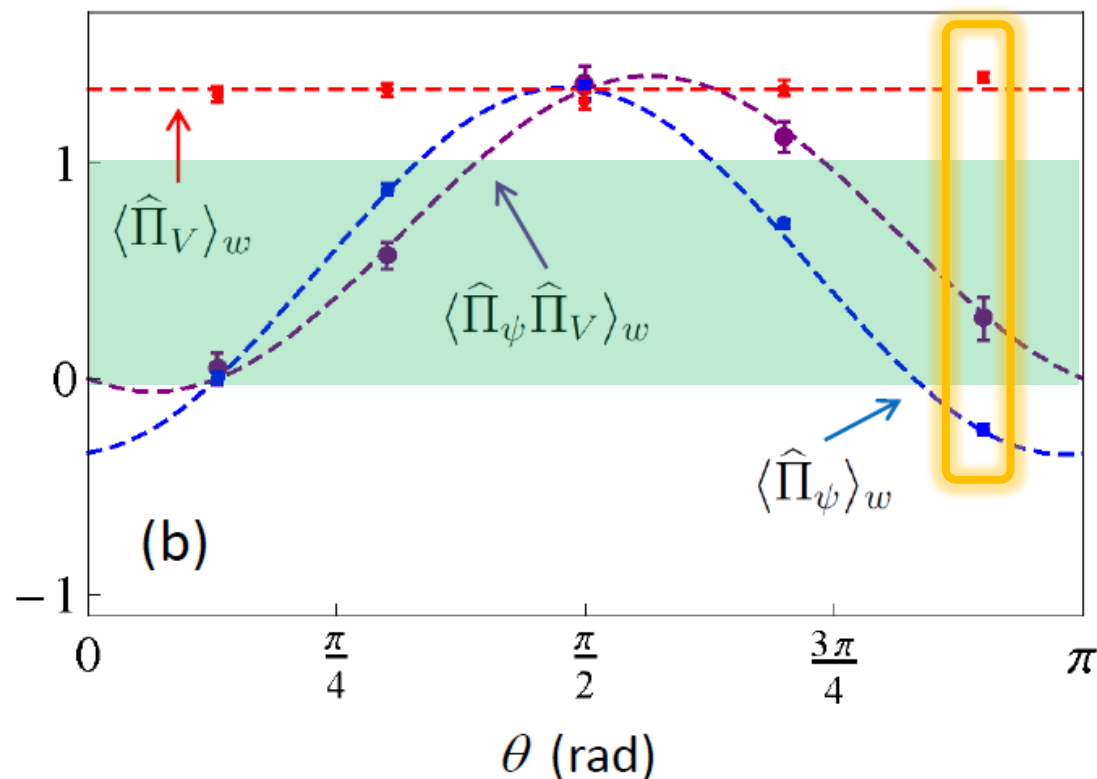
$$|\psi_i\rangle = 0.509|H\rangle + 0.861|V\rangle$$

$$|\psi_f\rangle = -0.397|H\rangle + 0.918|V\rangle$$

$$\langle\hat{\Pi}_V\rangle_w = 1.40(4)$$

$$\langle\hat{\Pi}_\psi\rangle_w = -0.24(3)$$

$$\langle\hat{\Pi}_\psi\hat{\Pi}_V\rangle_w = 0.28(10)$$



Piacentini et al., PRL 117, 170402 (2016)

Genetic Quantum Measurement

Estimating an expectation value by measuring a single photon

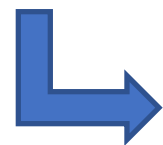
«Classical»-Coin-Tossing

Task: Investigation on the coins «fairness» produced by a mint (all coins are identical)

Probability of «head» in a single toss: β

In N trails the probability of having n «head» is: $B(n | N)$

The “fairness” of the mint production



Estimation of $\beta = \frac{\langle n \rangle}{N}$

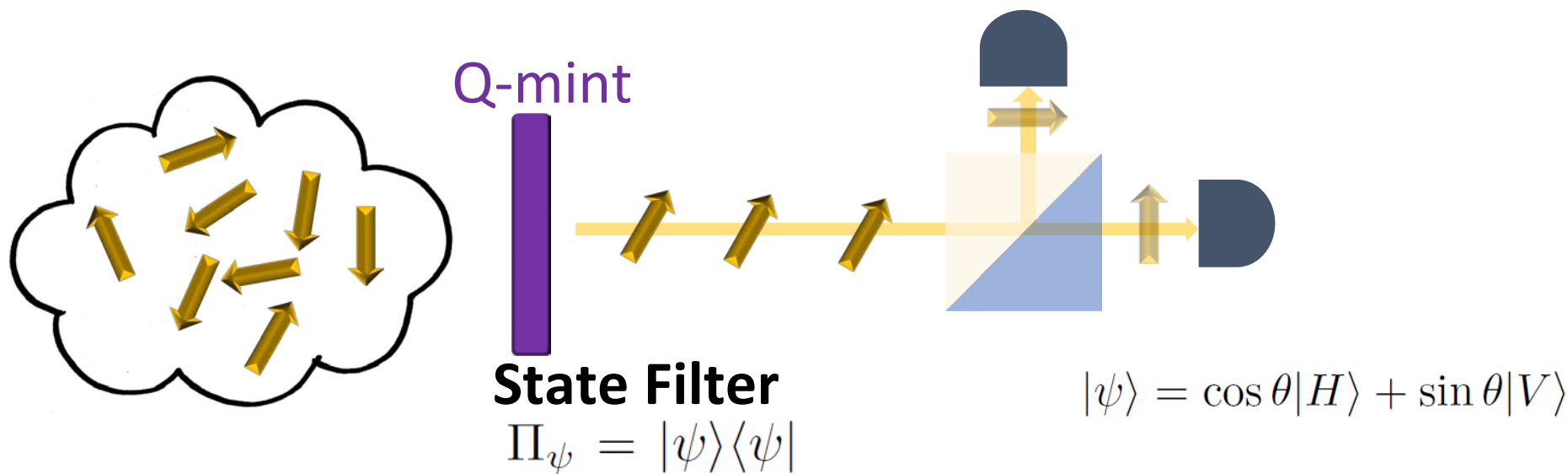
Uncertainty in the Estimation: $u_{\beta} = \sqrt{\frac{\beta(1-\beta)}{N}}$

Genetic Quantum Measurement

Estimating an expectation value by measuring a single photon

Quantum-Coin-Tossing

Task: Investigation on the Q-coins «fairness» produced by a Q-mint



The “fairness” of the Q-mint production: $P = |H\rangle\langle H| - |V\rangle\langle V|$

↳ $u_{\text{PBS}}(P) = \sqrt{\langle P^2 \rangle - \langle P \rangle^2} = \frac{|\sin(2\theta)|}{\sqrt{M}}$

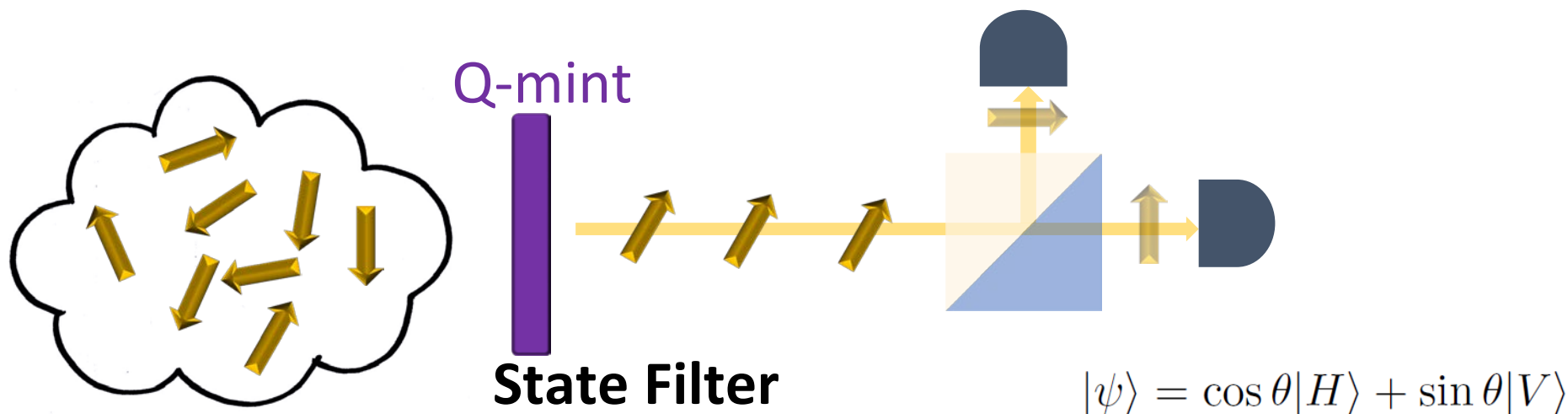
Equivalent to “classical” coin tossing

Genetic Quantum Measurement

Estimating an expectation value by measuring a single photon

Quantum-Coin-Tossing

Task: Investigation on the Q-coins «fairness» produced by a Q-mint



Quantum “weirdness” may help?

The Quantum-Cramer-Rao Bound: $u_{\text{QCR}}(P) \geq \frac{1}{\sqrt{M\mathcal{J}}}$

Q-Fisher Information: $\mathcal{J} = \frac{1}{|\sin(2\theta)|^2}$

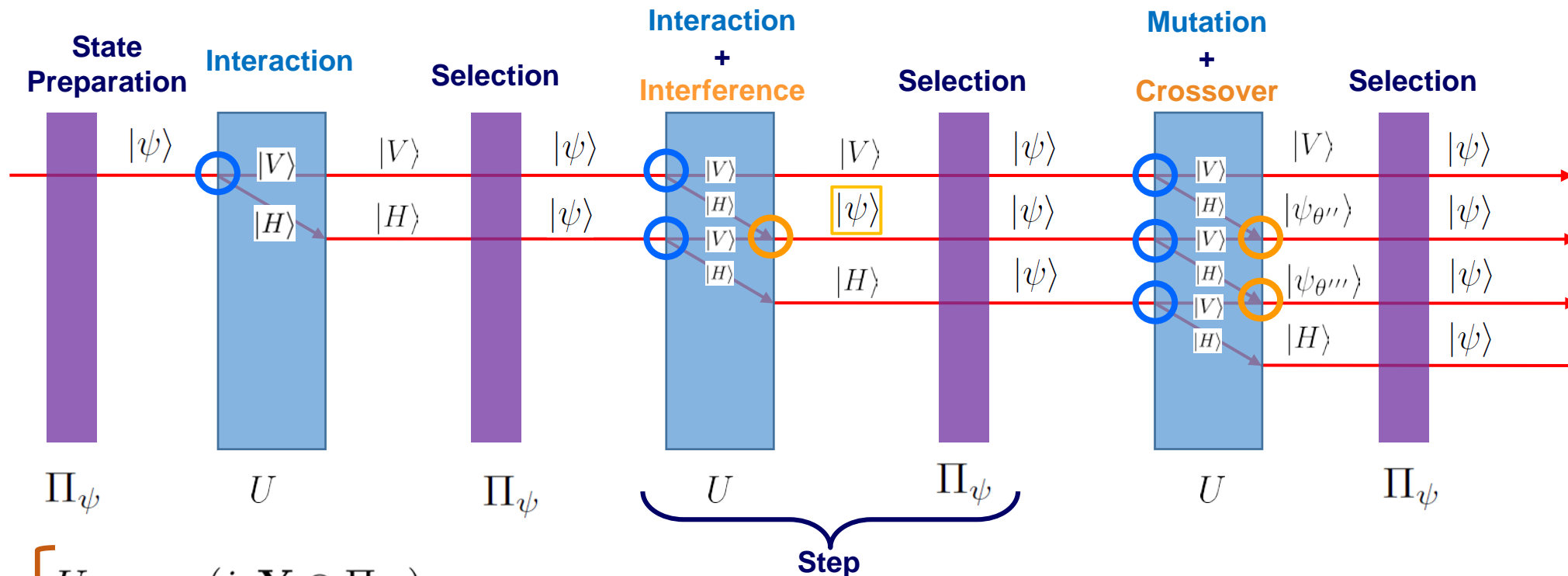
Equivalent to “classical” coin tossing



Genetic Quantum Measurement

Estimating an expectation value by measuring a single photon

GQM: a sequence of **identical steps** consisting of a **interaction-interference** stage and a **selection measurement** (equiv. state preparation)



$$\left\{ \begin{array}{l} U = \exp(ig\mathbf{Y} \otimes \Pi_H) \\ \Pi_\psi = |\psi\rangle\langle\psi| \end{array} \right.$$

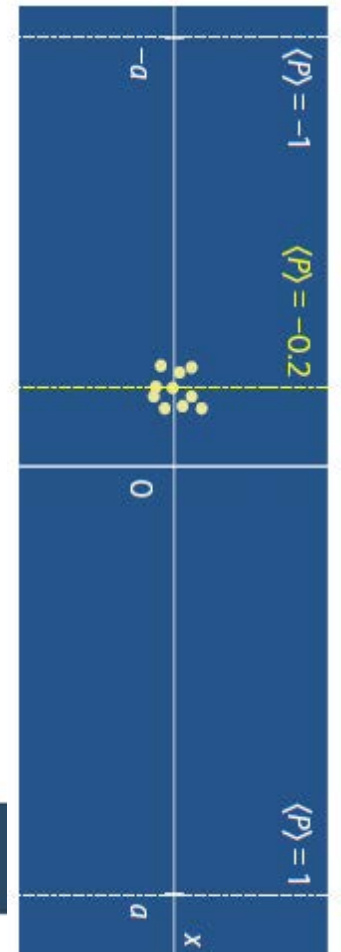
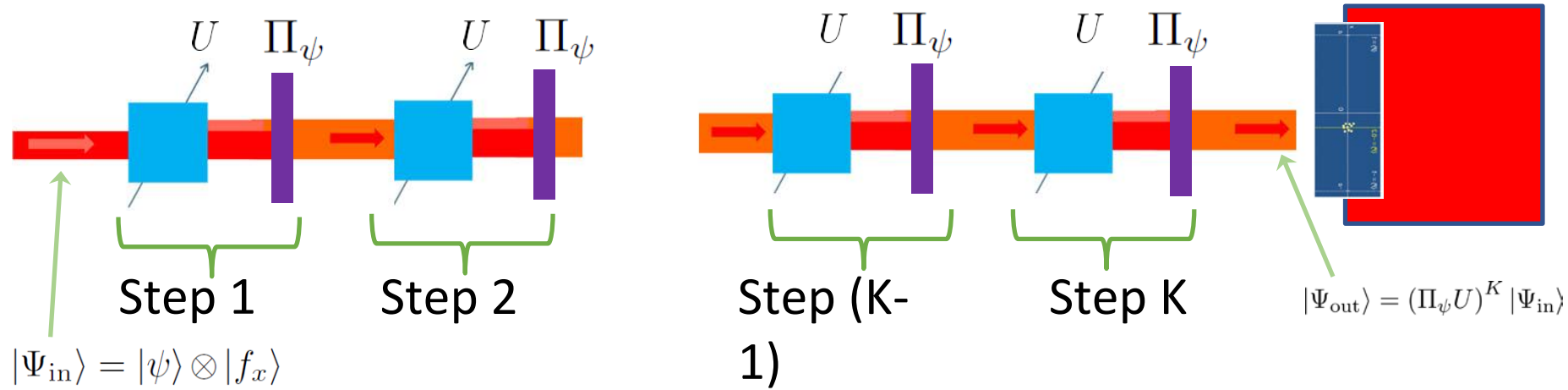
-) Group of **Selective** components (Q-mints) **assumed** identical
-) **Storage cavity** with a single Q-mint (e.g. PRL 103,163602)
-) ...

Nature Phys. **13**, 1191 (2017)



Genetic Quantum Measurement

Estimating an expectation value by measuring a single photon



The “fairness” of the Q-mint(s) production can be estimated by measuring the **expected value** of the **position** of the detected photons:

$$\epsilon(x) = \frac{Kg}{2} \langle P \rangle$$

with **uncertainty** $u(P) = u(x) \frac{2}{Kg}$

scaling with the number M of **detected** photons as: $M^{-1/2}$

$$P = |H\rangle\langle H| - |V\rangle\langle V|$$

$$u(x) = \sqrt{\epsilon(x^2) - \epsilon(x)^2}$$

$$\epsilon(x^n) = \int dx x^n F_K(x)$$

Genetic Quantum Measurement

Estimating an expectation value by measuring a single photon

Comparison between the uncertainty on P with the GQM approach ($u(P)$) and the one given by projective measurement ($u_{\text{PBS}}(P)$) with the **same number of initial photons, i.e.** M detected photons for the GQM; corresponding to $M p_{\text{sur}}(K)^{-1}$ initial photons both in t

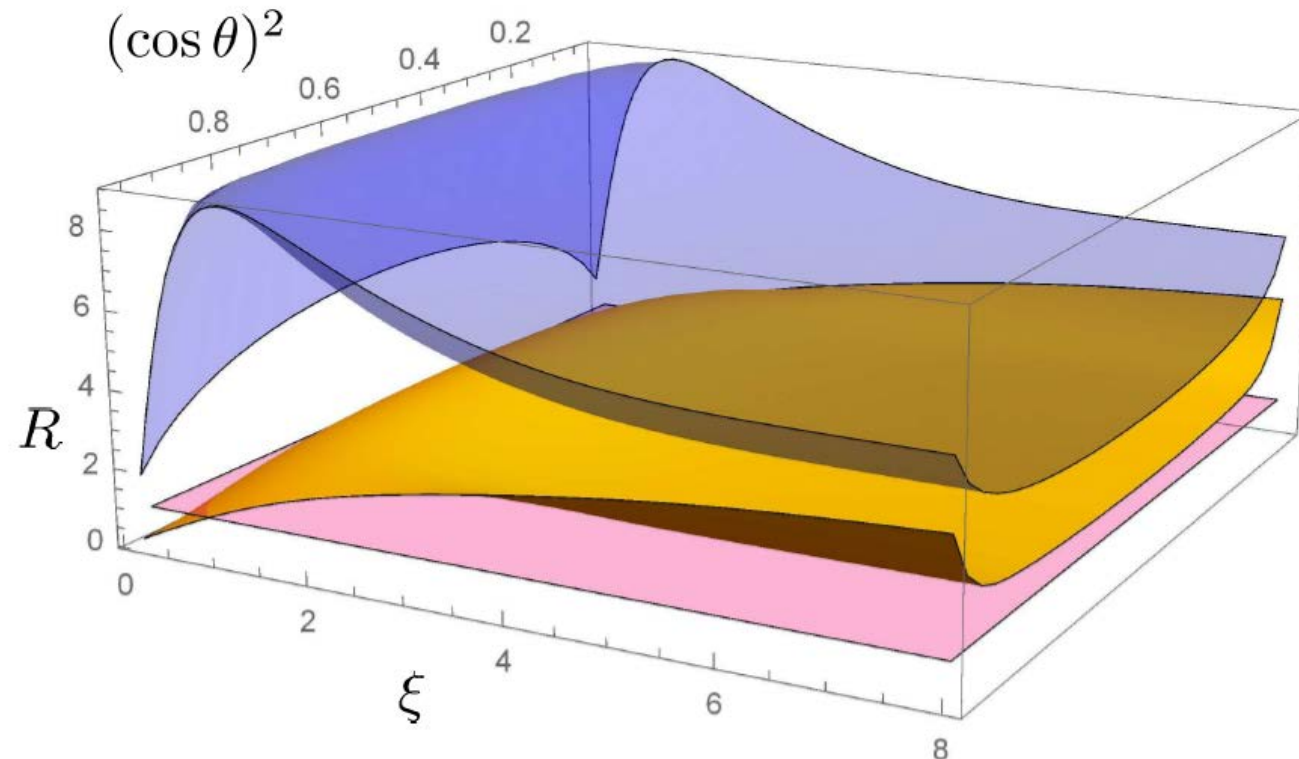
$$R = \frac{u_{\text{PBS}}(P)}{u(P)}$$

Yellow $K=7$

Blue $K=100$

Pink $R=1$

$$|\psi\rangle = \cos\theta|H\rangle + \sin\theta|V\rangle$$



$$\xi = g/\sigma$$

Genetic Quantum Measurement

Estimating an expectation value by measuring a single photon

Where this **extraordinary** superiority of **GQM** vs projective measurement **saturating QCR** bound comes from?

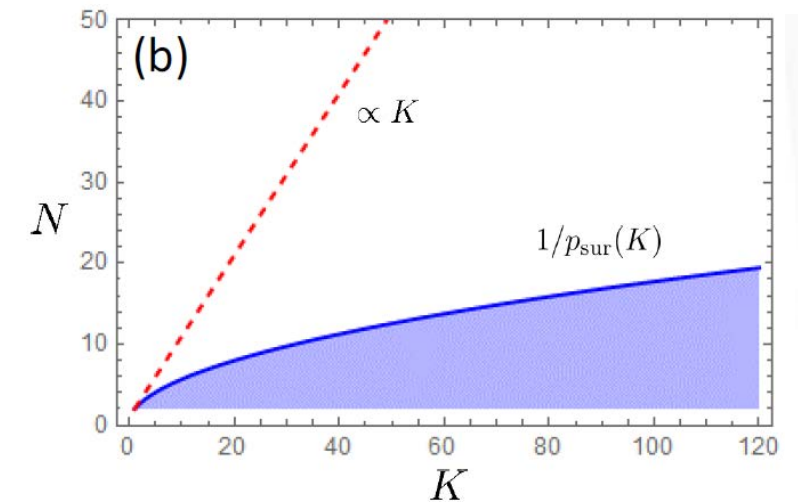
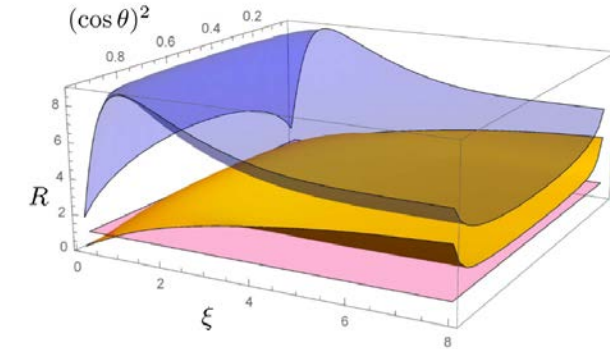
1) The uncertainty in **GQM** scales as $(NK)^{-1/2}$, while the number of initial photon used are $N/p_{\text{sur}}(K)$

2) **Q-CR Bound**. Fisher information associated to the POVM associated to the estimation of λ

$$F_X(\lambda) = \int d\nu \frac{[\partial_\lambda \text{tr}(\Pi(x)\rho_\nu)]^2}{\text{tr}(\Pi(x)\rho_\nu)}$$

The **optimal estimation** saturates $J(\lambda)$ (QFI) $F_X(\lambda) \leq J(\lambda)$

We are **outside** this framework since our POVM depends on the parameter to be estimate Π_λ ; because of the **selection**: Π_ψ

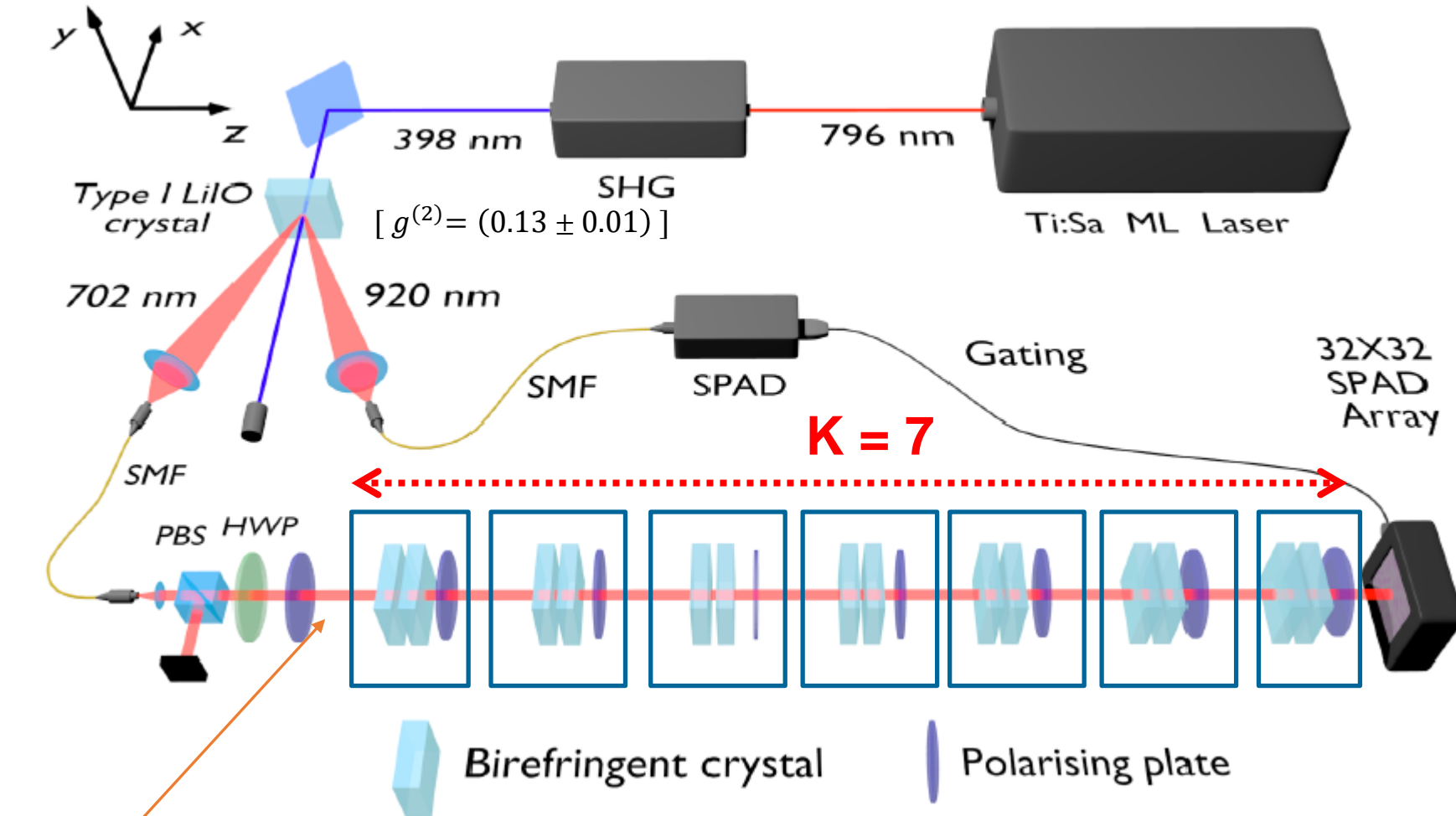


QUANTUM TECHNOLOGIES

INRiM
ISTITUTO NAZIONALE
DI RICERCA METROLOGICA

Genetic Quantum Measurement

Estimating an expectation value by measuring a single photon

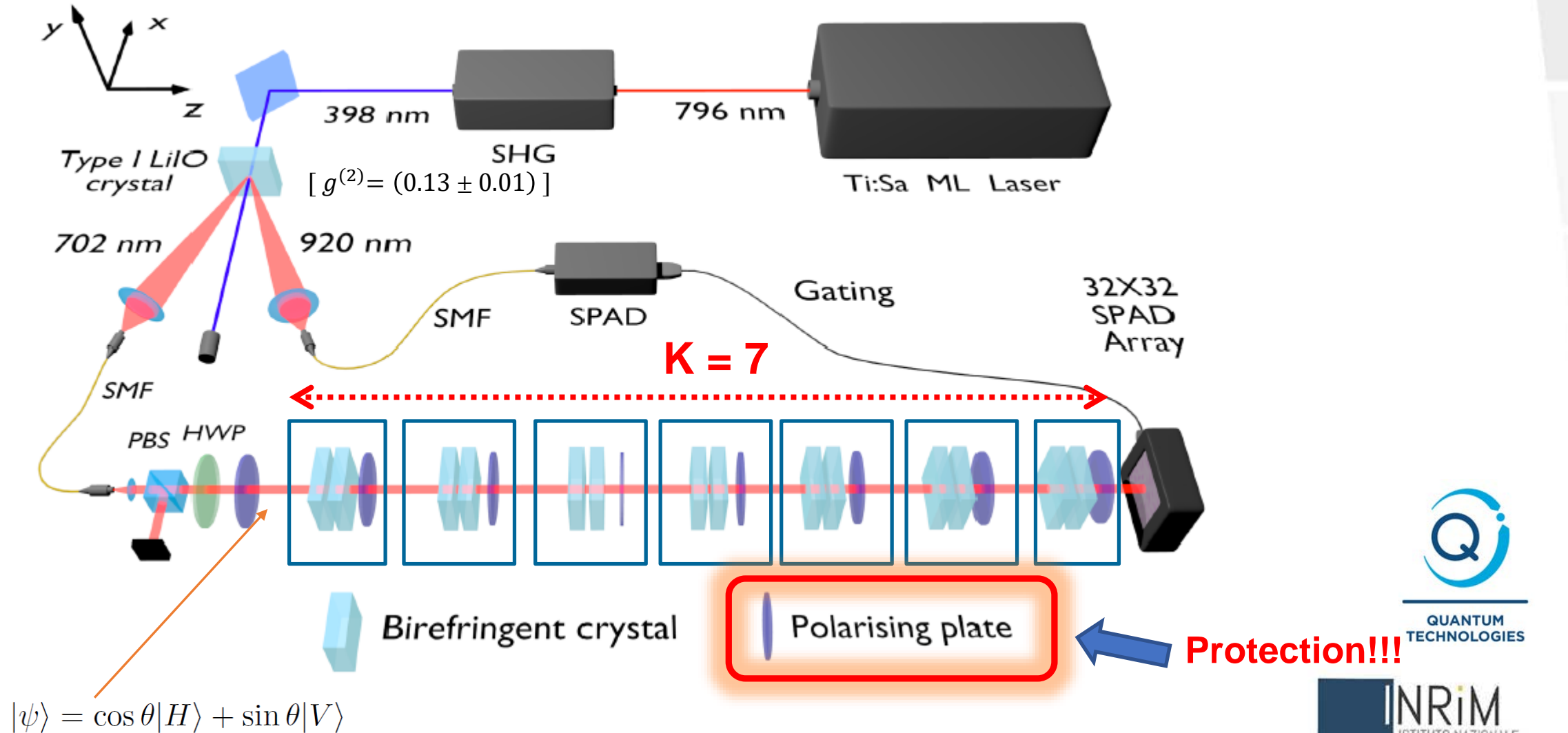


$$|\psi\rangle = \cos \theta |H\rangle + \sin \theta |V\rangle$$



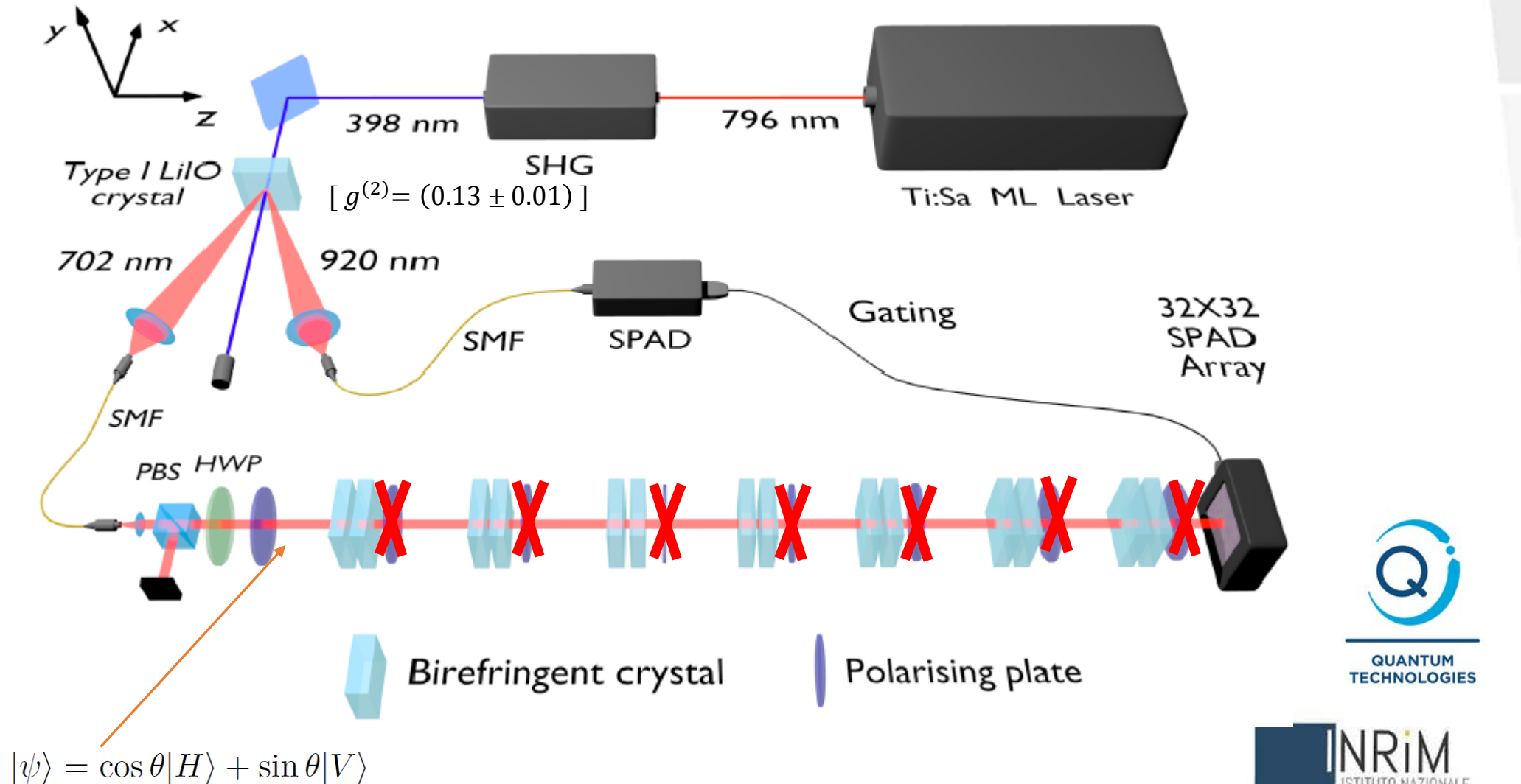
Genetic Quantum Measurement

Estimating an expectation value by measuring a single photon



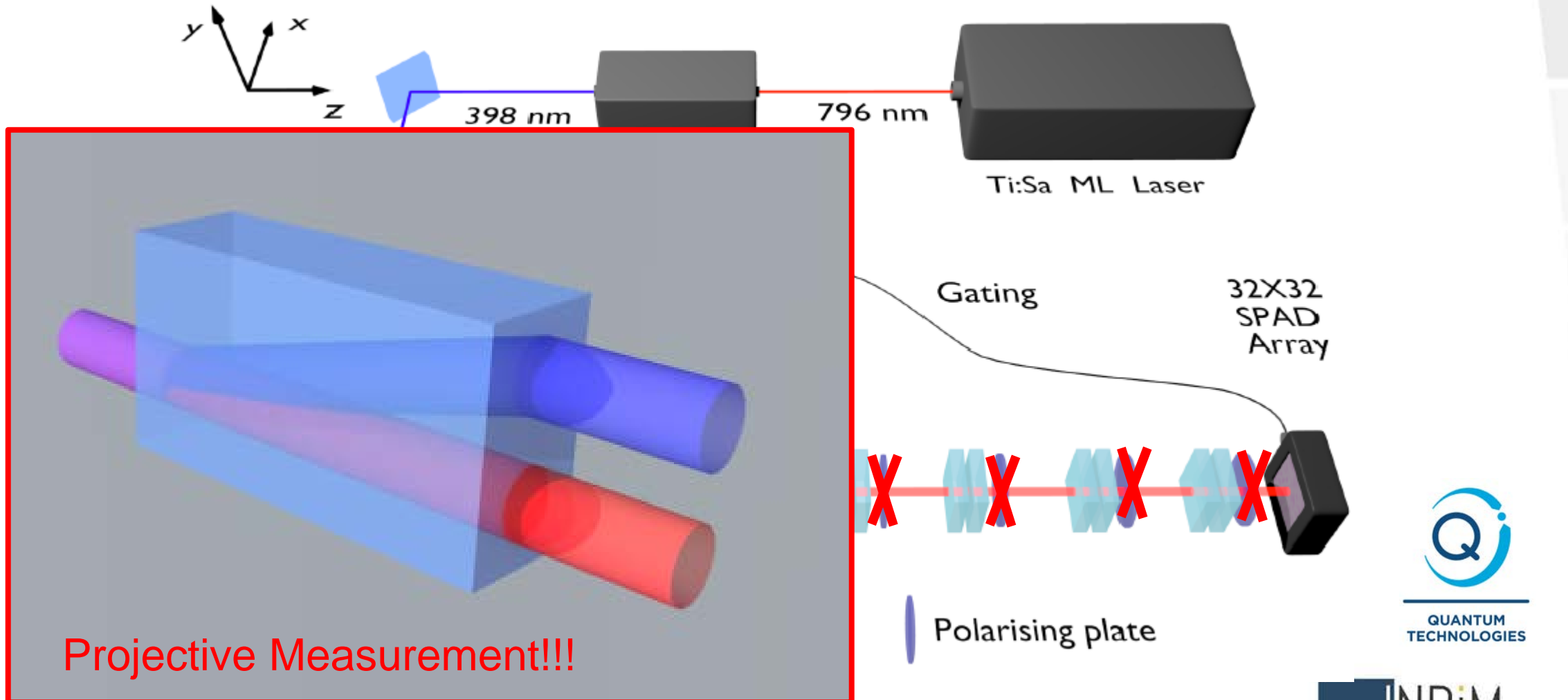
Genetic Quantum Measurement

Estimating an expectation value by measuring a single photon



Genetic Quantum Measurement

Estimating an expectation value by measuring a single photon



$$|\psi\rangle = \cos \theta |H\rangle + \sin \theta |V\rangle$$

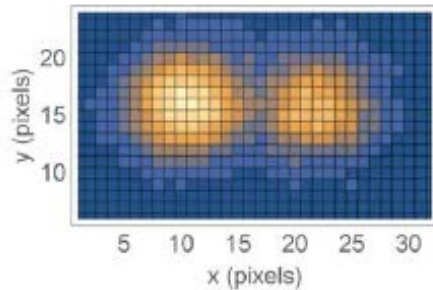


Genetic Quantum Measurement

Project.
Meas.

$$|\frac{17}{60}\pi\rangle = 0,629 |H\rangle + 0,777 |V\rangle$$

$$\langle P \rangle_{th} = -0,208$$

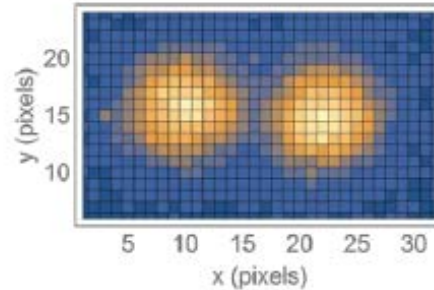


250 750 1250 1750 2250
counts / 1200 s

$$\langle P \rangle = -0,21(3)$$

$$|+\rangle = \frac{1}{\sqrt{2}} (|H\rangle + |V\rangle)$$

$$\langle P \rangle_{th} = 0$$

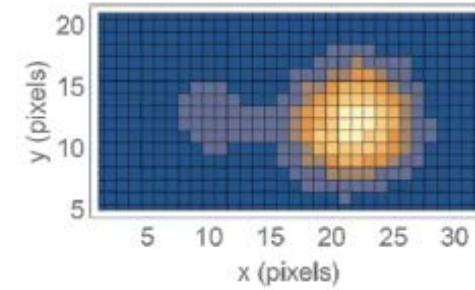


400 800 1200 1600 2000
counts / 1200 s

$$\langle P \rangle = -0,03(4)$$

$$|\frac{\pi}{8}\rangle = 0.924 |H\rangle + 0.383 |V\rangle$$

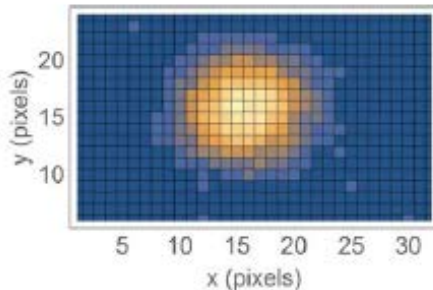
$$\langle P \rangle_{th} = 0,707$$



500 1000 1500 2000 2500 3000
counts / 1200 s

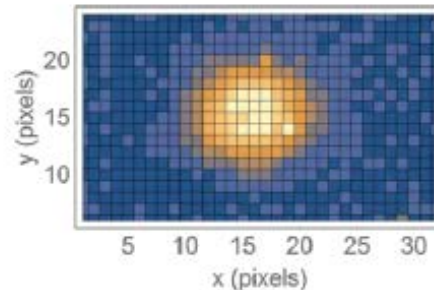
$$\langle P \rangle = 0,72(2)$$

GQM



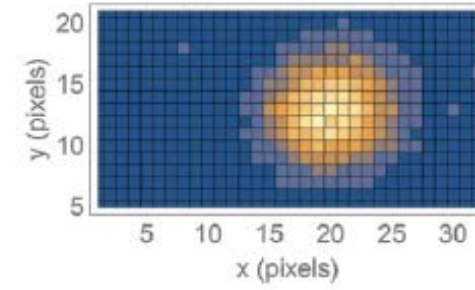
300 500 700 900 1100
counts / 1200 s

$$\langle P \rangle = -0,19(2)$$



300 500 700 900
counts / 1200 s

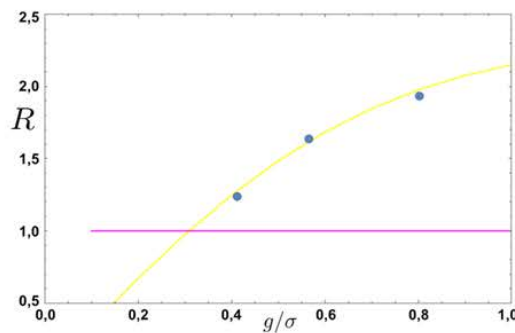
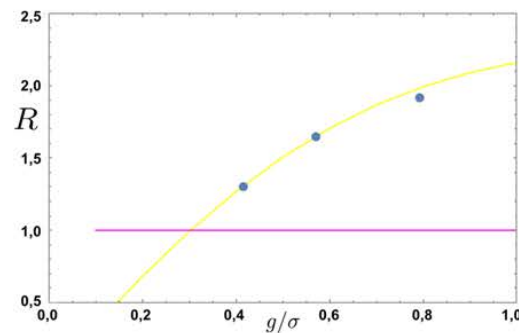
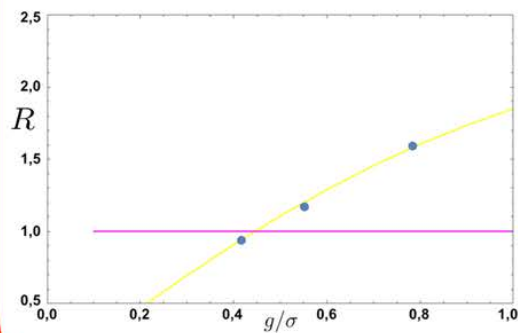
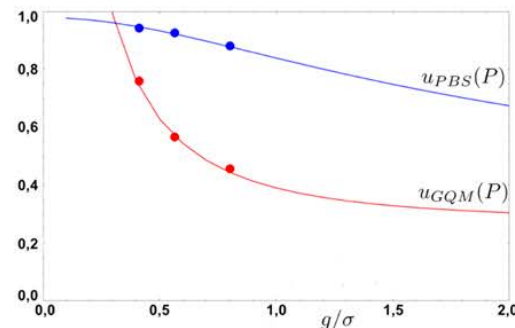
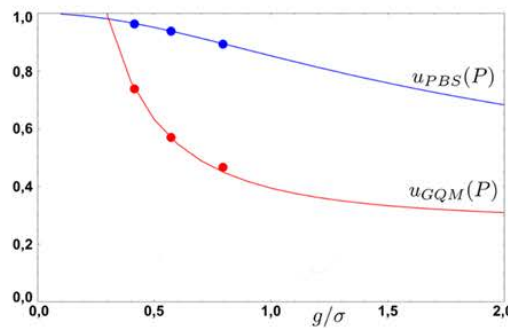
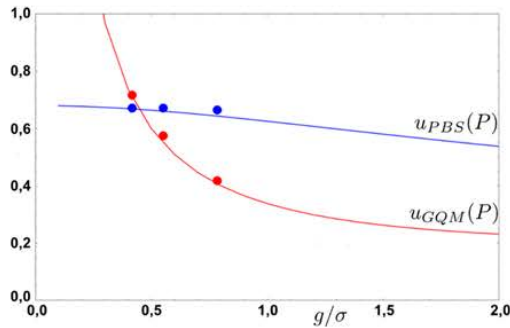
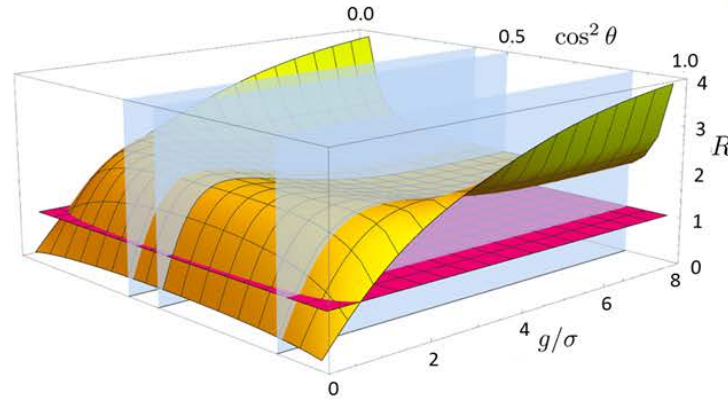
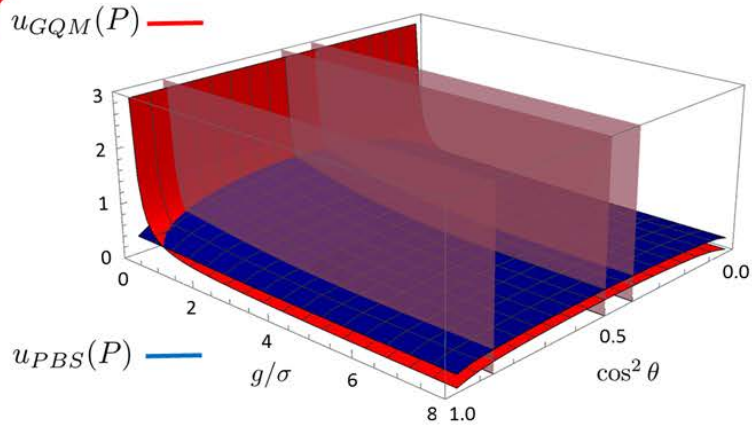
$$\langle P \rangle = 0,0012(14)$$



300 500 700 900
counts / 1200 s

$$\langle P \rangle = 0,72(2)$$

Genetic Quantum Measurement



$$|\psi_{\pi/8}\rangle = 0.924|H\rangle + 0.383|V\rangle$$

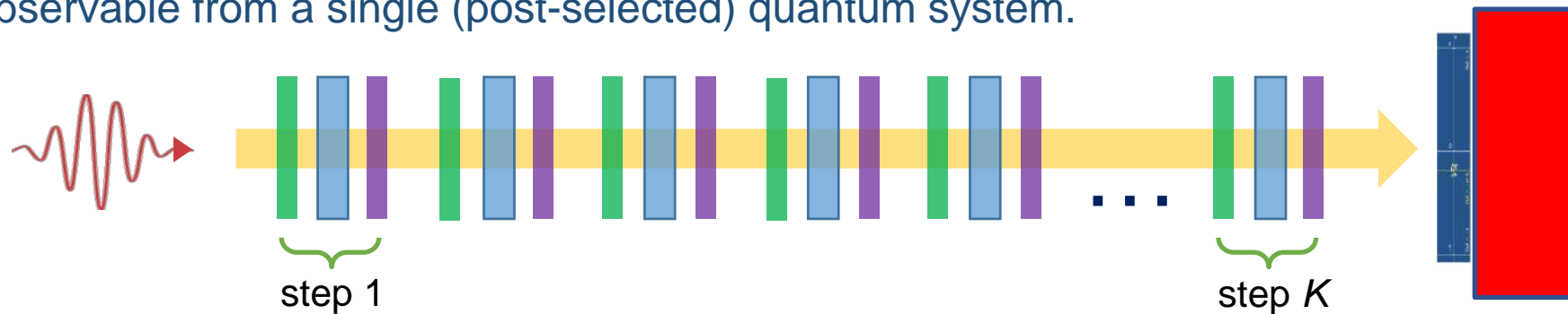
$$|\psi_{\pi/4}\rangle = \frac{1}{\sqrt{2}}(|H\rangle + |V\rangle)$$

$$|\psi_{\pi/8}\rangle = 0.629|H\rangle + 0.777|V\rangle$$

Robust Weak Measurement

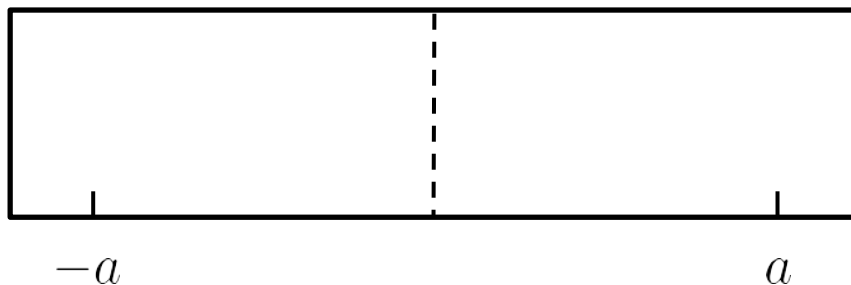
Weak values with a single measurement event

Robust Weak Measurement: iterative measurement protocol able to extract the weak value of an observable from a single (post-selected) quantum system.



Light: Sci. & Appl. **10**, 106 (2021)

Anomalous weak value:

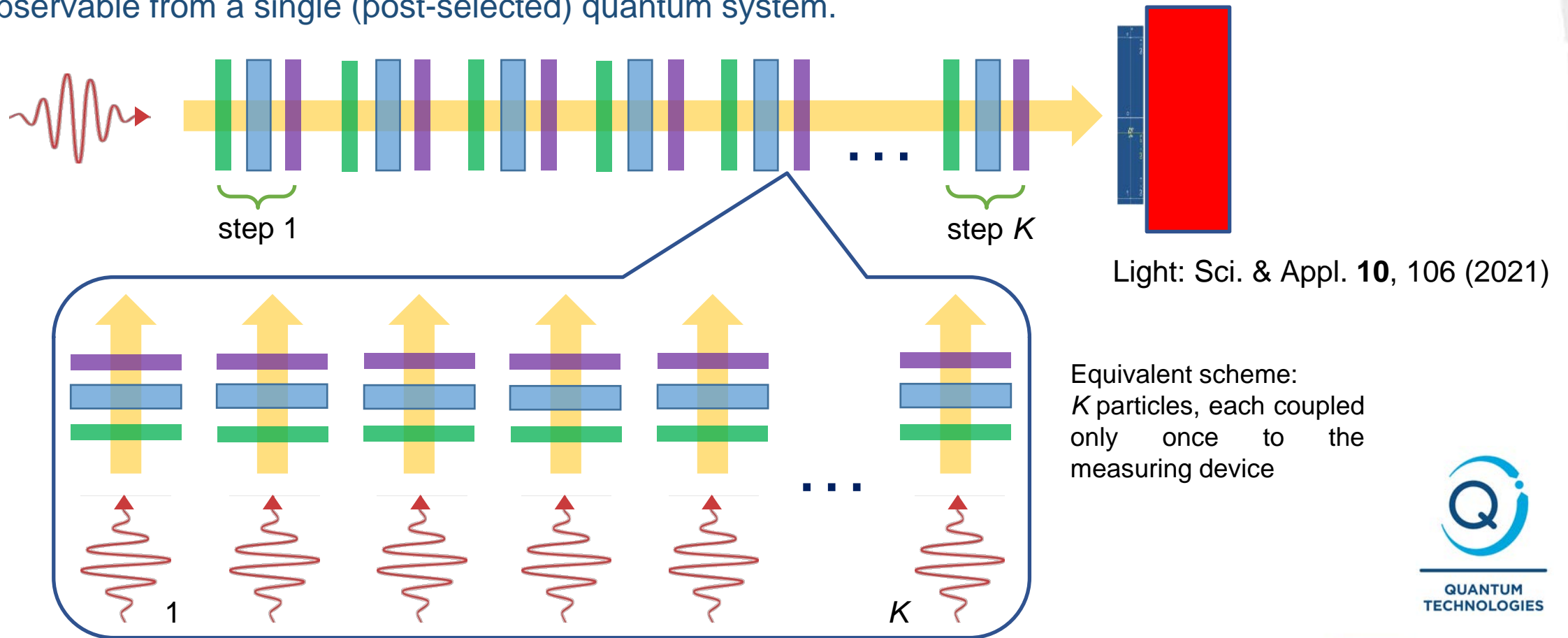


Light: S&A **10**, 106 (2021)

Robust Weak Measurement

Weak values with a single measurement event

Robust Weak Measurement: iterative measurement protocol able to extract the weak value of an observable from a single (post-selected) quantum system.



Measured observable:

$$\sigma_3^\Sigma \equiv \sum_{k=1}^K \sigma_3^{(k)} \quad \sigma_3^{(k)} = |H\rangle\langle H| - |V\rangle\langle V|$$



Light: S&A **10**, 106 (2021)

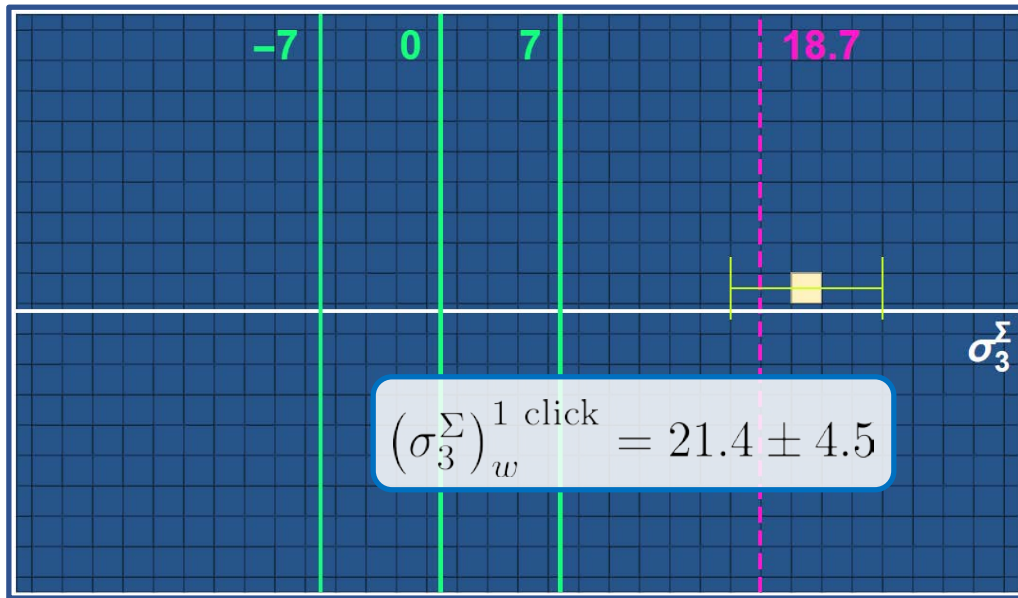
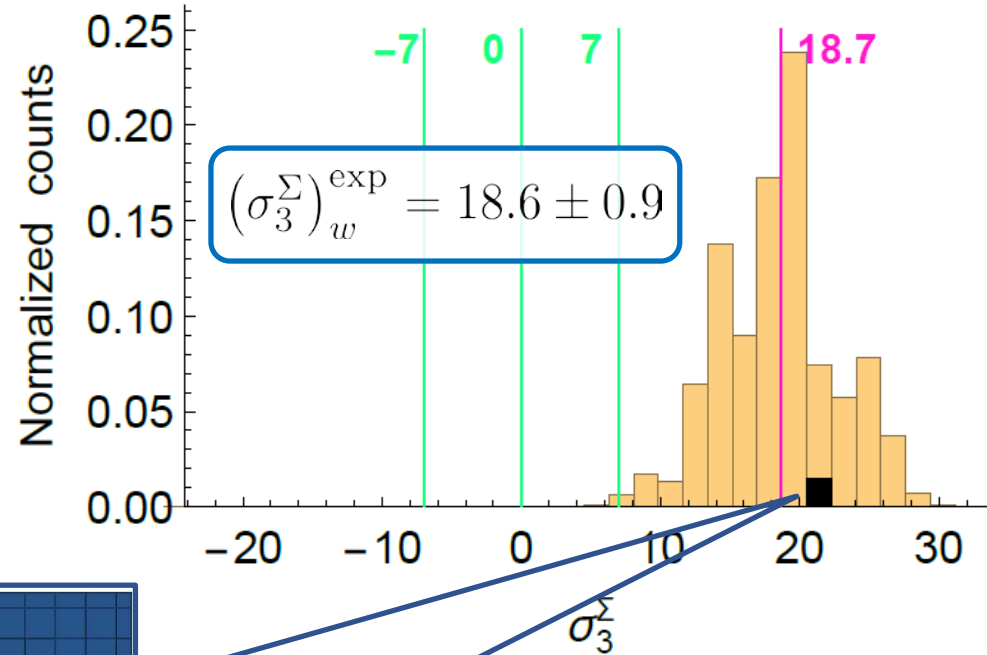
Robust Weak Measurement

Weak values with a single measurement event

$$|\psi_i\rangle = \cos \alpha |H\rangle + \sin \alpha |V\rangle$$

$$|\psi_f\rangle = \cos \beta |H\rangle + \sin \beta |V\rangle$$

α	0.62
β	2.53
g	0.17
$(\sigma_3^\Sigma)_w$	18.7



Our single click yields an anomalous value with a three standard deviations distance from the closest eigenvalue



**QUANTUM
TECHNOLOGIES**

... and this is not all ...



**QUANTUM
TECHNOLOGIES**

INRiM
ISTITUTO NAZIONALE
DI RICERCA METROLOGICA



**QUANTUM
TECHNOLOGIES**

... but it is enough for
today ...



**QUANTUM
TECHNOLOGIES**

INRiM
ISTITUTO NAZIONALE
DI RICERCA METROLOGICA



**QUANTUM
TECHNOLOGIES**

Thanks for your attention!



**QUANTUM
TECHNOLOGIES**

INRiM
ISTITUTO NAZIONALE
DI RICERCA METROLOGICA

A Avella	ED Lopaeva	V Schettini
E Bernardi	A Meda	A Shurupov
G Brida	MG Mingolla	C Stella
D Calonico	E Monticone	E Taralli
SA Castelletto	E Moreva	P Traina
A Cavanna	A Mura	S Virzì
L Ciavarella	C Novero	G Zanelli
C Clivati	G Petrini	M Zucco
Ivo Pietro Degiovanni	F Piacentini	
S Donadello	C Portesi	
M Genovese	ST Pradyumna	
M Gramegna	M Rajteri	
L Knoll	ML Rastello	
F Levi	E Rebufello	
MP Levi	I Ruo Berchera	
L Lolli	N Samantaray	

Thanks for your attention!

Collaborators

G Adesso, R Alléaume, UL Andersen, A Andreoni, A Bahgat Shehata, M Barbieri, J Bastie, M Bondani, FA Bovino, V Carabelli, G Castagnoli, TE Chapuran, MV Chekhova, E Cohen, M Colautti, AM Colla, CJ Chunnillall, A Della Frera, S Ditalia Tchernij, J Forneris, D Gatto Monticone, H Georgieva, T Gehring, A Ghazi-Bellouati, M Ghioni, P Giorda, N Gisin, A Giudice, EA Goldschmidt, A Gulinatti, T Herzig, ME Himbert, H Hofer, M Jaksic, CS Jacobsen, K Katamadze, G Kh Kitaeva, RA Kirkwood, S Kück, J Kupper, P Lombardi, M López, M Lucamarini, T Luhmann, R Lussana, N Lutkenhaus, G Margheri, C Marletto, V Martin, J Meijer, AL Migdall, A Mink, I Müller, S Olivares, P Olivero, MGA Paris, M Peev, S Pezzagna, M Pittaluga, SV Polyakov, G Porrovecchio, S Ragy, A Razet, SMF Raupach, E Rebufello, C Scarcella, A Shields, OA Shumilkina, N Skukan, AG Sinclair, G Tomagra, C Toninelli, A Tosi, M Trapuzzano, L Vaidman, V Vedral, F Villa, Z Yuan, M Ward, F Zappa, ...